Analysis of Geophysical Logs from Six Boreholes at Lariat Gulch, Former U.S. Air Force Site PJKS, Jefferson County, Colorado

By Frederick L. Paillet, Richard E. Hodges, and Barbara S. Corland

---

U.S. GEOLOGICAL SURVEY

Open-File Report 02–364

Prepared in cooperation with the
U.S. Air Force

Denver, Colorado
2002

U.S. DEPARTMENT OF THE INTERIOR
GALE A. NORTON, Secretary

U.S. GEOLOGICAL SURVEY
Charles G. Groat, Director

For additional information write to:

District Chief
U.S. Geological Survey
Box 25046, Mail Stop 415
Denver Federal Center
Denver, CO 80225–0046

Copies of this report can be purchased from:

U.S. Geological Survey
Information Services
Box 25286
Denver Federal Center
Denver, CO 80225

CONTENTS

FIGURES

TABLES

Analysis of Geophysical Logs from Six Boreholes at Lariat Gulch, Former U.S. Air Force Site PJKS, Jefferson County, Colorado

By Frederick L. Paillet, Richard E. Hodges, and Barbara S. Corland

ABSTRACT

This report presents and describes geophysical logs for six boreholes in Lariat Gulch, a topographic gulch at the former U.S. Air Force site PJKS in Jefferson County near Denver, Colorado. Geophysical logs include gamma, normal resistivity, fluid-column temperature and resistivity, caliper, televiewer, and heat-pulse flowmeter. These logs were run in two boreholes penetrating only the Fountain Formation of Pennsylvanian and Permian age (logged to depths of about 65 and 570 feet) and in four boreholes (logged to depths of about 342 to 742 feet) penetrating mostly the Fountain Formation and terminating in Precambrian crystalline rock, which underlies the Fountain Formation. Data from the logs were used to identify fractures and bedding planes and to locate the contact between the two formations. The logs indicated few fractures in the boreholes and gave no indication of higher transmissivity in the contact zone between the two formations. Transmissivities for all fractures in each borehole were estimated to be less than 2 feet squared per day.

INTRODUCTION

Water-quality-monitoring wells are routinely screened in a specified subsurface horizon, with screens installed along a narrow depth interval in order to relate water samples to specific aquifer zones. Without adequate information, well screens cannot be installed confidently along the intended aquifer zones. Driller's logs and descriptions of cuttings often are the only guidance available to ensure that the intended zones have been drilled and identified for screen installation. Geophysical well logs provide additional information on the condition of open boreholes if logs can be run in the period between drilling and well construction. The logs can be used to define the stratigraphic and structural conditions of the rock in the vicinity of the borehole and to indicate water-yielding intervals (Keys, 1990; Jorgensen, 1991; Paillet, Lundy, and others, 2000). The logs also place the interval designated for sampling within the larger hydrogeologic context of the aquifer at the study site. For example, the logs can indicate whether there are different water-quality zones present and whether different aquifer units are isolated from each other (Paillet and Crowder, 1996; Paillet, 2001). Such information can be of great use in interpreting the geochemical trends resulting from long-term water-quality monitoring (McCary, 1980; Kwader, 1985).

The work described in this report was done by the U.S. Geological Survey in cooperation with the U.S. Air Force. This report presents and describes geophysical logs obtained from six boreholes drilled during February–April 2002 for the installation of water-quality-sampling wells at Lariat Gulch in former U.S. Air Force site PJKS in Jefferson County, Colorado (fig. 1). The individual logs obtained in

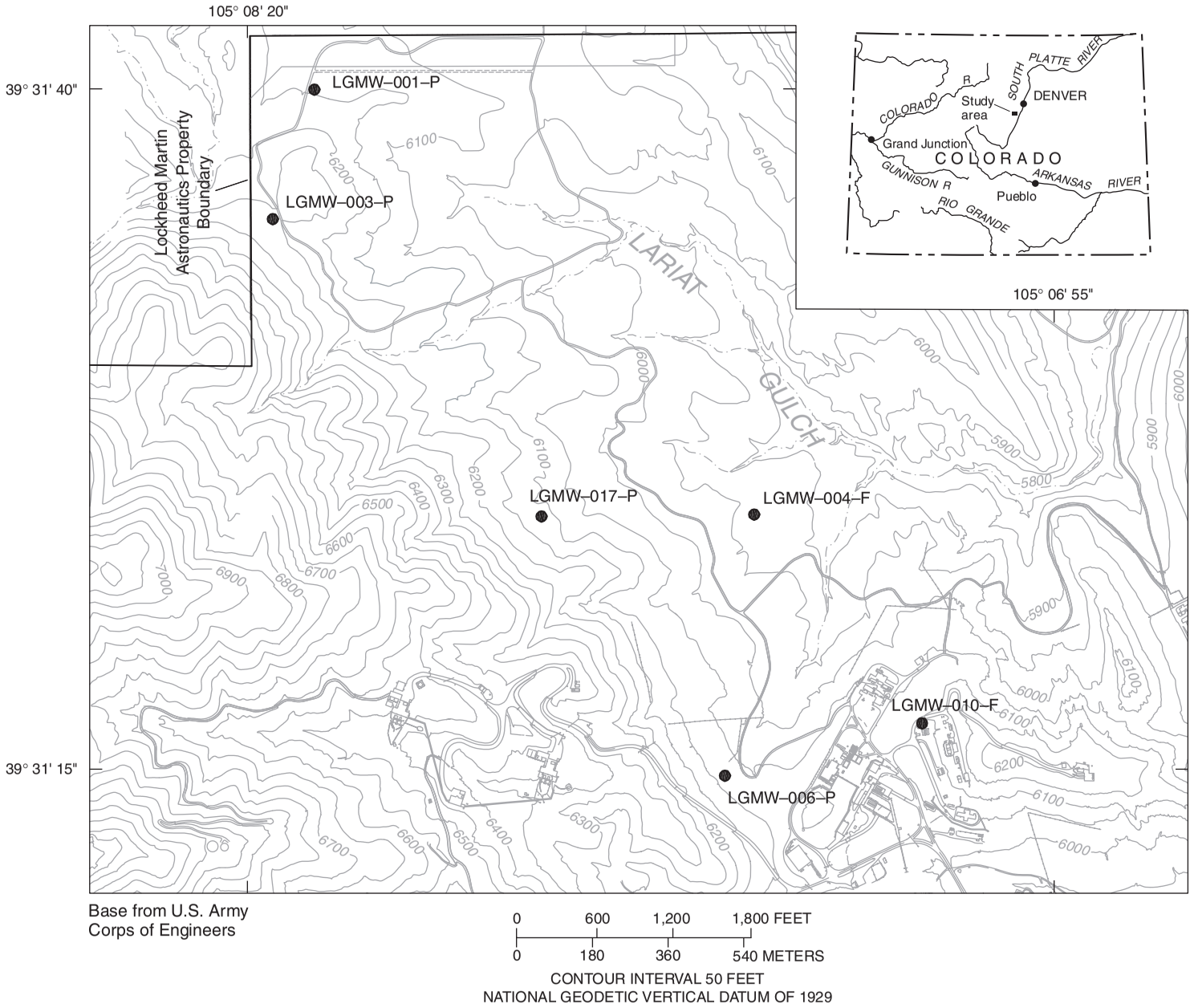

Figure 1. Lariat Gulch site showing locations of boreholes logged for this study.

each borehole are summarized in table 1. The two boreholes that terminated in the Fountain Formation were 65 and 570 feet deep. The four boreholes that terminated in Precambrian crystalline rocks were logged to 342–742 feet deep. The geophysical logs were used to guide well construction in Lariat Gulch.

Table 1. Summary of geophysical logs run in Lariat Gulch boreholes

[T, temperature; R, resistivity; boreholes suffixed with "P" terminate in Precambrian crystalline rocks; boreholes suffixed with an "F" terminate in the Fountain Formation]

Borehole	Log	Date	Comments
LGMW-001-P	Natural gamma	04–07–02	Open borehole below casing to 37 feet; well flowing and most walls obscured by mudcake; no data for flowmeter.
	Normal resistivity	04–07–02	
	Caliper	04–07–02	
	Acoustic televiewer	04–07–02	
	Fluid-column T and R	04–07–02	
LGMW-003-P	Natural gamma	03–20–02	Open borehole below recovering water level.
	Normal resistivity	03–20–02	
	Caliper	03–20–02	
	Acoustic televiewer	03–20–02	
	Heat-pulse flowmeter	03–20–02	
	Fluid-column T and R	03–20–02	
LGMW-004-F	Natural gamma	03–04–02	Open borehole below recovering water level.
	Normal resistivity	03–04–02	
	Caliper	03–04–02	
	Acoustic televiewer	03–04–02	
	Heat-pulse flowmeter	03–04–02	
	Fluid-column T and R	03–04–02	
LGMW-006-P	Natural gamma	03–19–02	Open borehole below recovering water level.
	Normal resistivity	03–19–02	
	Caliper	03–19–02	
	Acoustic televiewer	03–19–02	
	Heat-pulse flowmeter	03–19–02	
	Fluid-column T and R	03–19–02	
LGMW-010-F	Natural gamma	02–20–02	Open borehole below recovering water level; probable convection in borehole. Flowmeter data not usable.
	Normal resistivity	02–20–02	
	Caliper	02–20–02	
	Acoustic televiewer	02–20–02	
	Heat-pulse flowmeter	02–20–02	
LGMW-017-P	Natural gamma	04–05–02	Open borehole below recovering water level.
	Normal resistivity	04–05–02	
	Caliper	04–05–02	
	Acoustic televiewer	04–05–02	
	Heat-pulse flowmeter	04–05–02	
	Fluid-column T and R	04–05–02	

Parsons Engineering Science, Inc. (1999a) described the study area of this report. Lariat Gulch (fig. 1) is a topographic gulch located in and north of former U.S. Air Force site PJKS in Jefferson County, Colorado, about 20 miles south-southwest of Denver. The 460-acre PJKS site was constructed in 1956–57 inside the boundaries of the property of Lockheed Martin Astronautics (formerly Martin Marietta Astronautics Group) for research and testing related to rockets. During operations, facilities on the ridge on the south side of Lariat Gulch contaminated ground water, primarily with trichloroethylene (TCE). In February 2001, the PJKS site was deeded to Lockheed Martin Astronautics; the U.S. Air Force retained responsibility for environmental restoration.

Geophysical logs described in this report were run in boreholes drilled into the Precambrian crystalline rocks and the Fountain Formation of Pennsylvanian and Permian age. Parsons Engineering Science, Inc. (1999b) described the Precambrian rocks in the vicinity of Lariat Gulch as amphibolite, migmatite, and gneissic quartz monzonite or granodiorite and the Fountain Formation as alternating and intercalated silty sandstone and irregular siltstone lenses. Outcrop width and dip angles indicate that the Fountain Formation, which rests unconformably on the Precambrian crystalline rocks, is approximately 3,000 feet thick in the vicinity of Lariat Gulch. Geophysical logs in this report for boreholes suffixed with an "F" (LGMW-004-F and LGMW-010-F) are only in the Fountain Formation; those suffixed with a "P" (LGMW-001-P, LGMW-003-P, LGMW-006-P, and LGMW-017-P) are mostly in the Fountain Formation and terminate short distances (about 40 to 60 feet) into the Precambrian rocks.

BACKGROUND ON GEOPHYSICAL LOGS

Geophysical well logs provide profiles of the physical properties of formations surrounding boreholes (Keys, 1986, 1990; Paillet and Crowder, 1996). Some of these logs (gamma and normal resistivity) can be related to the volume averaged over a region surrounding the probe. Other logs provide properties of the fluid column within the borehole (fluid-column temperature and resistivity) or of the formation where it intersects the borehole wall (caliper and televiewer). The heat-pulse flowmeter provides direct information about the location of inflow zones in boreholes. General information about the analysis of geophysical logs in ground-water studies can be found by consulting general references such as Hearst and others (2000) and Keys (1990). The specific geophysical logs used in this study are described in the following sections.

Natural Gamma

The gamma log (fig. 2) gives a measure of the natural gamma activity of a sample volume approximately 1 foot in diameter surrounding a gamma detector in the logging probe (Keys, 1986, 1990). The gamma activity given by the probe in counts per second is a relative value, depending upon the size, efficiency, and shielding of the detector. Gamma counts are also subject to random fluctuations related to nuclear statistics. These fluctuations are removed from the data set by averaging the response of the detector over periods long enough to give an effective average of the gamma production in the sample volume. The average gamma activity of a formation is related to the proportion of the radioisotopes of the naturally occurring elements uranium, potassium, and thorium that occur in the minerals composing the formation. This log can be obtained in water-filled or air-filled boreholes and in boreholes cased with plastic or steel pipe where allowance is made for the partial shielding provided by the casing.

Normal Resistivity

The normal-resistivity log (fig. 2) measures the resistivity of the formation around the logging probe by means of an alternating current applied to the region around the probe (Keys, 1990). The electrode spacing

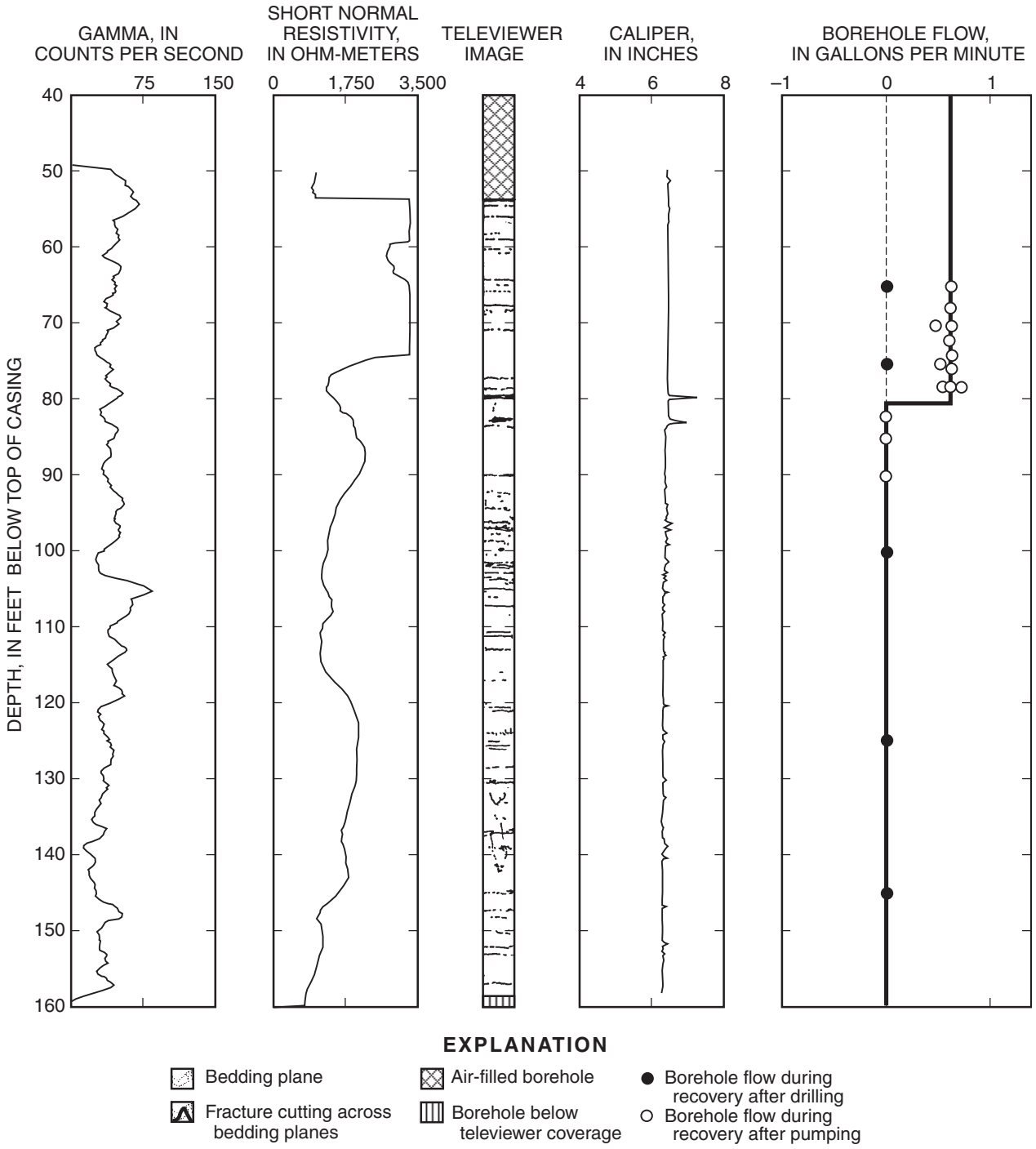

Figure 2. Example of gamma, resistivity, televiewer, caliper, and borehole-flow logs.

(for example, short or 16 inches and long or 64 inches) determines the size of the sample volume. Resistivity logs cannot be run in air-filled or cased boreholes. The normal-resistivity log is run in open, fluid-filled boreholes.

Fluid Column

The fluid-column log measures the temperature and electrical resistivity of the fluid filling the borehole. If the borehole has been static and undisturbed for a substantial period of time, the diffusion of solutes ensures that the electrical resistivity of the fluid column becomes uniform and that the temperature of the fluid column conforms to the local geothermal gradient. If water flows between zones in the borehole, abrupt changes in slope in the resistivity or temperature profiles may indicate the depth intervals where water is entering or exiting the borehole (Keys, 1990; Paillet, 2000a).

Acoustic Televiewer

The acoustic-televiewer log provides a magnetically oriented image of the pattern of ultrasonic reflectivity of the borehole wall (Williams and Johnson, 2000; Paillet and others, 1985; Zemanek and others, 1970). The orientation (strike and dip) and relative aperture of each fracture can be estimated from the televiewer image (fig. 3). Because fracture aperture typically is enlarged by drilling and because the thin fracture intersection is smeared by imaging with an approximately 0.4-inch-wide ultrasonic beam, the image gives a qualitative and not a quantitative estimate of local fracture aperture. The acoustic-televiewer probe used for this study contains a borehole deviation sensor that allows logging system software to automatically correct the televiewer log for the departure of the borehole axis from vertical in the computation of fracture strike and dip. Local magnetic declination is subtracted from the measured strike because the televiewer interpretation is based on magnetic (not geographical) north. The acoustic televiewer can only be operated in a fluid-filled borehole. The pulse frequency of the ultrasonic source determines the diameter range over which the probe can be used. The televiewer used in this study has a nominal upper limit of 9 inches for borehole diameter, but this limit may be reduced slightly if mud reduces the speed of sound in the borehole fluid. The muddy borehole water precluded use of an optical televiewer in Lariat Gulch boreholes.

Televiewer logs indicate the presence of planar features intersecting the borehole wall because the rough nature of the rock at the intersection scatters acoustic energy, while the adjacent rock serves as a uniform reflecting surface. The geometry of the image indicates whether it conforms to the expected sinusoidal shape of a plane intersecting a cylindrical borehole. Such planes can be lithologic contrasts, bedding planes, bedding planes opened by solution, or true fractures. In cases where a sedimentary strike and dip or foliation can be recognized in the logs (as in this study), borehole-wall openings that clearly cut across these bedding planes are interpreted as fractures. Apparent planar openings in the borehole that are roughly parallel to sedimentary fabric or foliation are interpreted as bedding-plane openings. In either case, the log indicates only that the bedding plane or fracture has been enlarged in the immediate vicinity of the borehole wall. For example, Paillet and others (1985) demonstrate that permeable fractures intersecting boreholes may be impossible to distinguish from sealed fractures where infilling minerals have been eroded by the drilling process. Paillet (1998) and Paillet and others (1987) also show that the apparent size of fracture openings as given by televiewer and caliper logs does not correlate with fracture permeability as quantified by straddle-packer tests.

Caliper

The caliper log (fig. 2) gives the average diameter of the borehole in inches based on the deflection of three spring-loaded arms as the probe is moved upward in the borehole (Keys, 1990). The relative diameter of the borehole given by the caliper log is related to the hardness of the formation and the

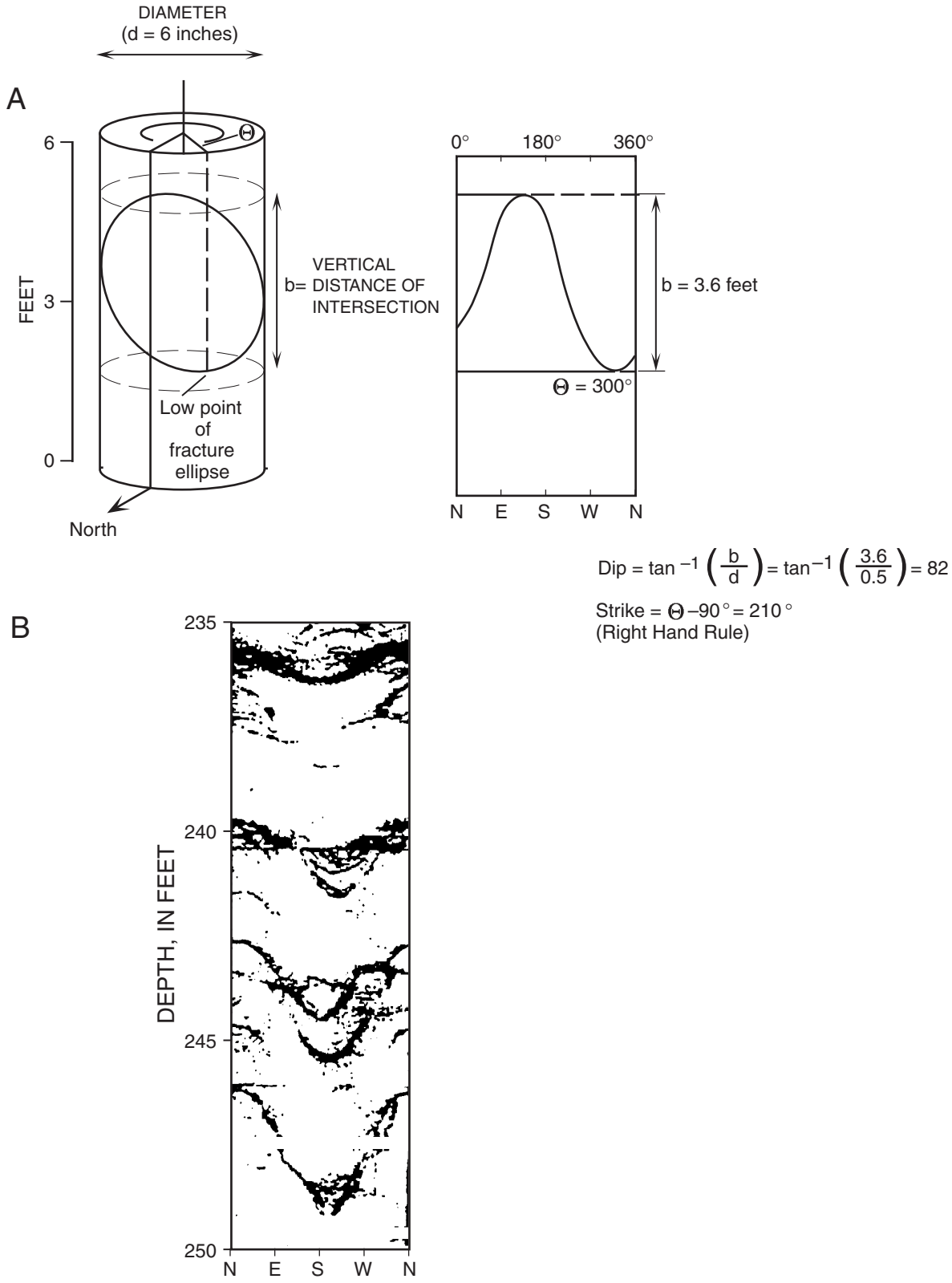

Figure 3. Example of acoustic-televiewer log indicating how fracture strike and dip are interpreted from the televiewer-log image.

presence of structural features such as bedding planes or fractures that locally weaken the borehole wall. This log can be run in air or water-filled boreholes and will measure the inside diameter of the casing when run in a cased borehole.

Heat-Pulse Flowmeter

The heat-pulse flowmeter measures the time required for a small thermal pulse induced at a wire grid to move up or down to either of a pair of thermistors located about 0.8 inch above and below the grid (Hess, 1986; Paillet and others, 1987). The pulse traveltime is calibrated to flow rates in laboratory columns (fig. 4). However, the flowmeter only measures the flow through the cylindrical measurement section of the probe. Additional flow may bypass the flowmeter in the annular region between the probe and the borehole wall. A flexible-disk flow diverter is installed on the flowmeter to block the flow in the annulus. However, some leakage of flow around the diverter always occurs and must be accounted for in a field calibration, as described by Paillet (2000a). Heat-pulse flowmeter measurements are made with the probe stationed at discrete depth intervals between possible inflow or outflow zones in the borehole. Differences in flow measurements can be used to determine the amount of flow entering or exiting the borehole in the intervals between points of flow measurement (fig. 2).

Quality Control

In general, quality control of geophysical logs obtained for water-quality studies is based on the experience and professional practice of the geophysicist (Paillet and Crowder, 1996; American Society for Testing and Materials, 1995). The single most important check is by an experienced log analyst who determines if the logs from any borehole have all of the qualities attributed to acceptable data. Such data attributes include indications of major formation contacts, water level, bottom of casing (if present), and physical property values (gamma activity, formation resistivity, and so forth) that appear reasonable for the local hydrogeologic environment. Other experience relates to knowledge of calibration methods, the frequency with which specific probes are known to drift out of calibration, and warmup times required to prevent thermal drift in probe response caused by changes in internal temperature of probe electronics. In addition to these general, experience-related aspects of quality control, several specific quality-control topics are addressed in all geophysical logging studies, as described by Hodges (1988), Keys (1990), Hodges and Teasdale (1991), and the American Society for Testing and Materials (1995). Logs in this report are within the limits of acceptable error.

Analysis

The geophysical logs collected at the Lariat Gulch site were analyzed using accepted log-interpretation methods, as described by McCary (1980), Keys (1986), and Paillet and Crowder (1996). The log analysis was divided into separate areas of analysis, as described in the following paragraphs.

Lithology

In analyzing the suite of geophysical logs run for this project, the gamma and resistivity logs can be related to formation lithology. According to standard geophysical-log interpretation references (Hearst and others, 2000; Paillet and Crowder, 1996; Keys, 1990), the natural gamma activity and resistivity of geologic formations vary with the specific minerals in the rock fabric. Formation resistivity also depends upon the electrical resistivity of the water in porous rocks (Kwader, 1985). The gamma activity of sedimentary formations increases with the amount

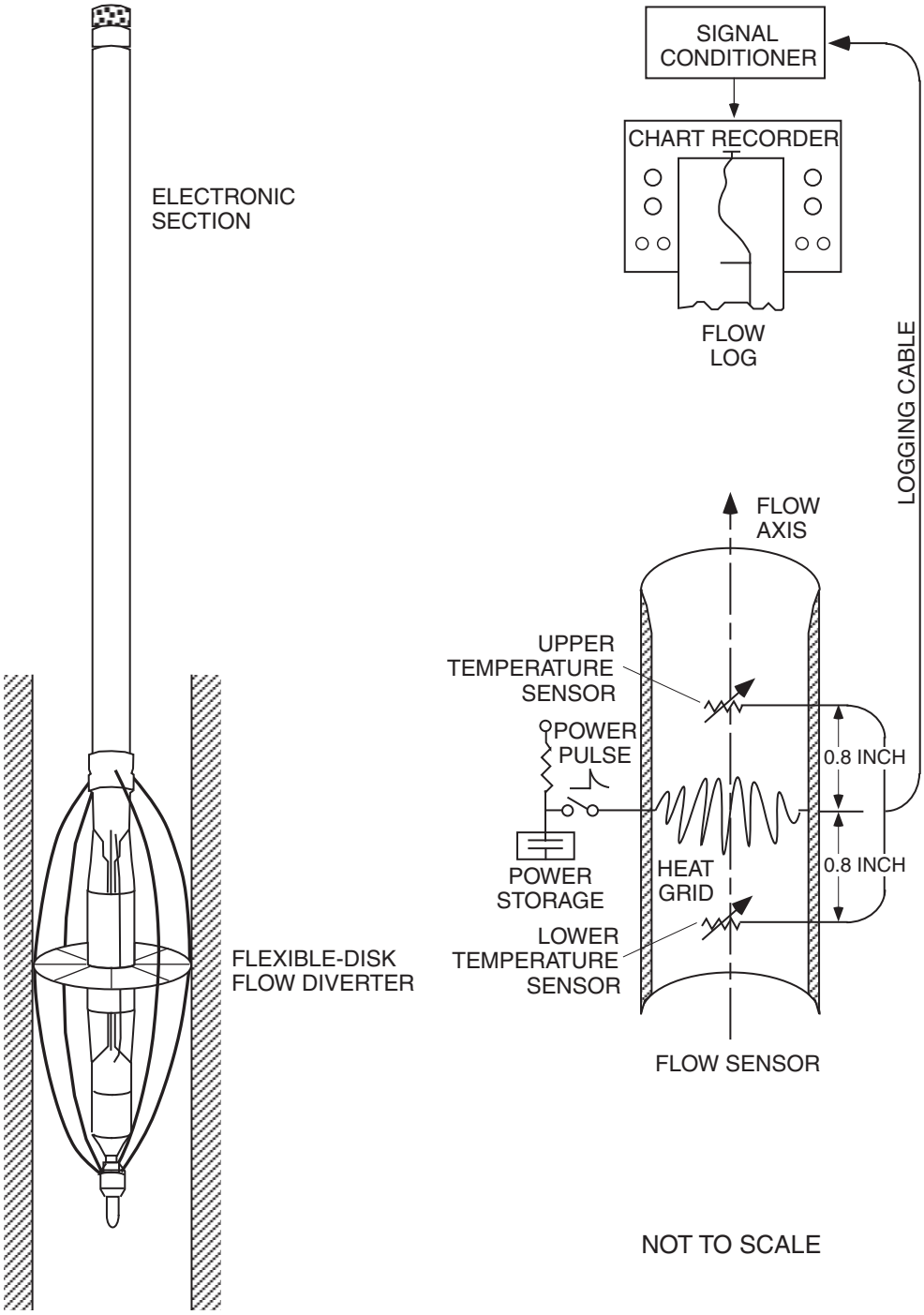

Figure 4. Schematic illustration of the heat-pulse flowmeter.

of clay minerals present and decreases with the proportion of clastic mineral grains. The gamma activity of crystalline rock formations increases with the proportion of potassium feldspar present and generally is high for granitic basement rocks. In freshwater-bearing formations, the electrical resistivity of pore water generally is negligible and contributes relatively little to bulk formation electrical resistivity.

Structure

Borehole televiewer image and caliper logs indicate the depth and orientation of beds, lithologic contacts, and fractures that intersect the borehole. The televiewer indicates planelike features intersecting the borehole wall. It is impossible to positively identify many of these features as bed contacts, bedding openings, or fractures. In this study, structural features identified on televiewer logs were separated into two classes: (1) bedding planes having a relatively consistent orientation throughout the borehole, and (2) fractures having variable orientations that are seen to cut across bedding planes in the televiewer log image. The televiewer-data-analysis software incorporates a measure of borehole deviation so that bedding-plane and fracture orientations are picked with respect to the borehole axis and are automatically corrected to a true vertical coordinate system. The televiewer software picks the vertical dip and the azimuth of the downdip intersection of the feature and the borehole. Because the orientation is given with respect to local magnetic north, the strike of each bedding plane or fracture was corrected true north to account for the local magnetic declination (13 degrees east of true north).

Heat-Pulse Flowmeter

Almost all geophysical well logs produce measurements that are indirectly related to hydraulic properties of interest to the hydrogeologist, such as formation porosity and permeability. These geophysical logs are converted to estimates of hydrogeologic properties through various theoretical or empirical equations. High-resolution flowmeter logs, such as those obtained with the heat-pulse flowmeter, are an exception to this rule because these logs can be used to directly estimate in-situ formation permeability. Under ideal conditions, flowmeter-log data can be used to determine the transmissivity and hydraulic head of each water-producing interval in a borehole. Two steady or quasi-steady flow profiles obtained under two different conditions (usually ambient and steady-pumping conditions) are used either to eliminate the effect of hydraulic head from the analysis by the subtraction-of-inflows method (Morin and others, 1988; Molz and others, 1989) or to solve for both zone transmissivity and hydraulic head of each inflow zone by a flow-modeling method (Paillet, 1998, 2000a).

Drilling operations required completion of test wells shortly after drilling, before water levels had stabilized in boreholes. Under this limitation, most boreholes were logged while water levels were recovering from dewatering by air-rotary drilling. Pumping was conducted for short periods to increase drawdown or to allow additional measurements in the water-level-recovery mode, but sufficient time was not available in the drilling schedule to make flowmeter measurements under stabilized drawdown conditions. Because hydraulic-head conditions changed throughout the flow-measurement period, borehole-flow data were normalized and presented as if they were obtained under a constant drawdown of 25 feet. Once the flow data were normalized, the flowmeter-log data could be used to give a qualitative or semiquantitative analysis of the hydraulic conditions in the vicinity of the borehole. The data could be used to identify the depth intervals where water was entering the borehole. The flowmeter-log data also could be used to identify crossflow, where some of the water entering the borehole exits elsewhere in the borehole. Such crossflow conditions indicate differences in hydraulic head between zones, although the magnitude of the head differences could not be estimated from the data.

Flowmeter-Measurement Adjustments and Normalization

In this study, flowmeter measurements were made at discrete depth stations. This approach maximizes the sensitivity of the flowmeter in low-flow environments (Paillet, 2000a) and does not require the correction of data

to eliminate flow bias introduced by continuous motion of the probe during measuring (Paillet, Lundy, and others, 2000). Borehole-flow measurements are given in the form of heat-pulse-transit times within the measurement section of the probe. These values are calibrated in units of flow through the measurement section of the probe by using flow-column calibration in the laboratory (Hess, 1986). These calibrated data are then subject to two corrections: (1) correction to account for leakage of flow around the flexible disk used to seal the annulus between the probe and the rough borehole wall, and (2) correction to account for substantial changes in drawdown during the measurement period. Each of these corrections was carried out as follows:

1. The bypass around the probe is estimated using a bypass factor (Paillet, 2000b; Paillet, Senay, and others, 2000). The measured flow given by the flowmeter is multiplied by the bypass factor to give total borehole flow. The bypass factor is estimated by comparing the measured flow with known flow. In many studies, the bypass factor is estimated by comparing the known pumping rate to flow measurements during pumping in the interval above all inflow zones. In this study, measured flow data were compared with the rate of borehole recovery in the interval just below the water level during water-level recovery. For example, a measured rate of water-level recovery of about 10 feet per hour would correspond with an upward flow of about 0.43 gallon per minute (gpm) of water in an 8-inch-diameter borehole. Virtually all flow measurements made in this study involved values close to the 0.01-gpm limit for measurement of flow by the heat-pulse flowmeter, causing relatively large variation in replicate measurements. The bypass factor was estimated by taking the average value for the data sets in the four boreholes where meaningful flow profiles were obtained. For example, the upward flow of water in borehole LGMW-004-F was given as 0.05 gpm by the average of measurements ranging from less than 0.01 to about 0.10 over a period when the average upward flow determined from water-level recovery was about 0.25 gpm. Thus, the bypass factor was found to be about 5.0, which falls within the range of bypass factors estimated in other flowmeter studies involving the same kind of flexible-disk flow diverter in rough-walled boreholes.
2. The effect of changing drawdown during the measurement period was eliminated from the flow data by normalizing the flow measurements to coincide with a standard drawdown condition. Thus, the flowmeter data were corrected to give the flow expected to occur at a standard 25 feet of drawdown instead of the actual drawdown at the time of measurement. This normalization required an estimate of the drawdown at the time of each flow measurement: the time at the start of each flow measurement was recorded, and the drawdown at that time was estimated by fitting a continuous curve to the discrete water-level measurements made during the logging period. An estimate of the final static water level in the borehole was made by projecting the recovery to steady state. This curve was used to estimate the drawdown at each measurement period. Then, the rate of upward flow of water in the borehole was assumed to be proportional to the drawdown at any given time.

In order to do these two corrections, data were converted to give total borehole flow at normalized drawdown conditions using the following equation:

$$Q = B_f Q_0 (d/d_0) \tag{1}$$

where

Q is the total borehole flow estimated at the measurement station under the standard drawdown of 25 feet,
B_f is the bypass factor (assigned a value of 5.0 for this study),
Q_0 is the flow measurement given by the calibrated response of the flowmeter in the laboratory flow column,
d is the drawdown at the time of measurement, and
d_0 is the standard drawdown of 25 feet.

INTERPRETATION OF LARIAT GULCH LOGS

Six boreholes were logged at the Lariat Gulch site during February–April 2002. A summary of the logs run in each borehole is given in table 1. Composites of the logs for each borehole are given in figures 5A–10A; the composite logs present a suite of measurements consisting of gamma, formation resistivity, fluid-column temperature and resistivity, caliper, televiewer, and heat-pulse flowmeter. The deviation of each borehole from vertical is plotted in figures 5B–10B. Because of the consolidated lithology and fresh ground water, the short-normal log was run for the measurement of formation resistivity.

Bedding planes and fractures were imaged by acoustic televiewer in five of six boreholes (excluding LGMW-001-P). The top of televiewer log in all plots was at the water level in the borehole. The presence of mud derived from formation clays in the bottom of boreholes precluded the televiewer logging near the bottom of some boreholes and probably affected the fluid-column-resistivity logs in these deeper intervals by altering (probably increasing) fluid resistivity, which could not be corrected.

Openings intersecting the borehole were divided into three classes: (1) bedding planes and bedding-plane fractures, (2) fractures cutting across bedding planes in the Fountain Formation or across rock foliation in the basement rocks, and (3) irregular "washouts" and borehole enlargements of unknown nature. The orientation of bedding planes (strike and dip) in the Fountain Formation as derived from the televiewer log images is summarized in table 2. Strike and dip of fractures are summarized in table 3.

Five of the six boreholes were logged with the heat-pulse flowmeter during recovery of water level after drilling; borehole LGMW-001-P was not logged because of the presence of a thick mudcake on the wall of the borehole. Water-level measurements made during recovery after dewatering during air-rotary drilling and during recovery after the water level was drawn down by pumping are listed in table 4. The discrete-depth flow measurements and the corrected (normalized) flow values derived from those measurements are summarized in table 5. In all cases, water-level recovery was very slow and amounted to corrected upflow (upward flow of water in the borehole) rates of less than 0.9 gpm at drawdown averaging 10–30 feet. Upflow rates during recovery were so slow that steady pumping could not be sustained in any of the boreholes. A submersible pump was used to draw down water levels for one repeated recovery-flow test in boreholes LGMW-004-F, LGMW-006-P, and LGMW-017-P. Specific comments on the borehole flow data for each of the boreholes are given in the following sections.

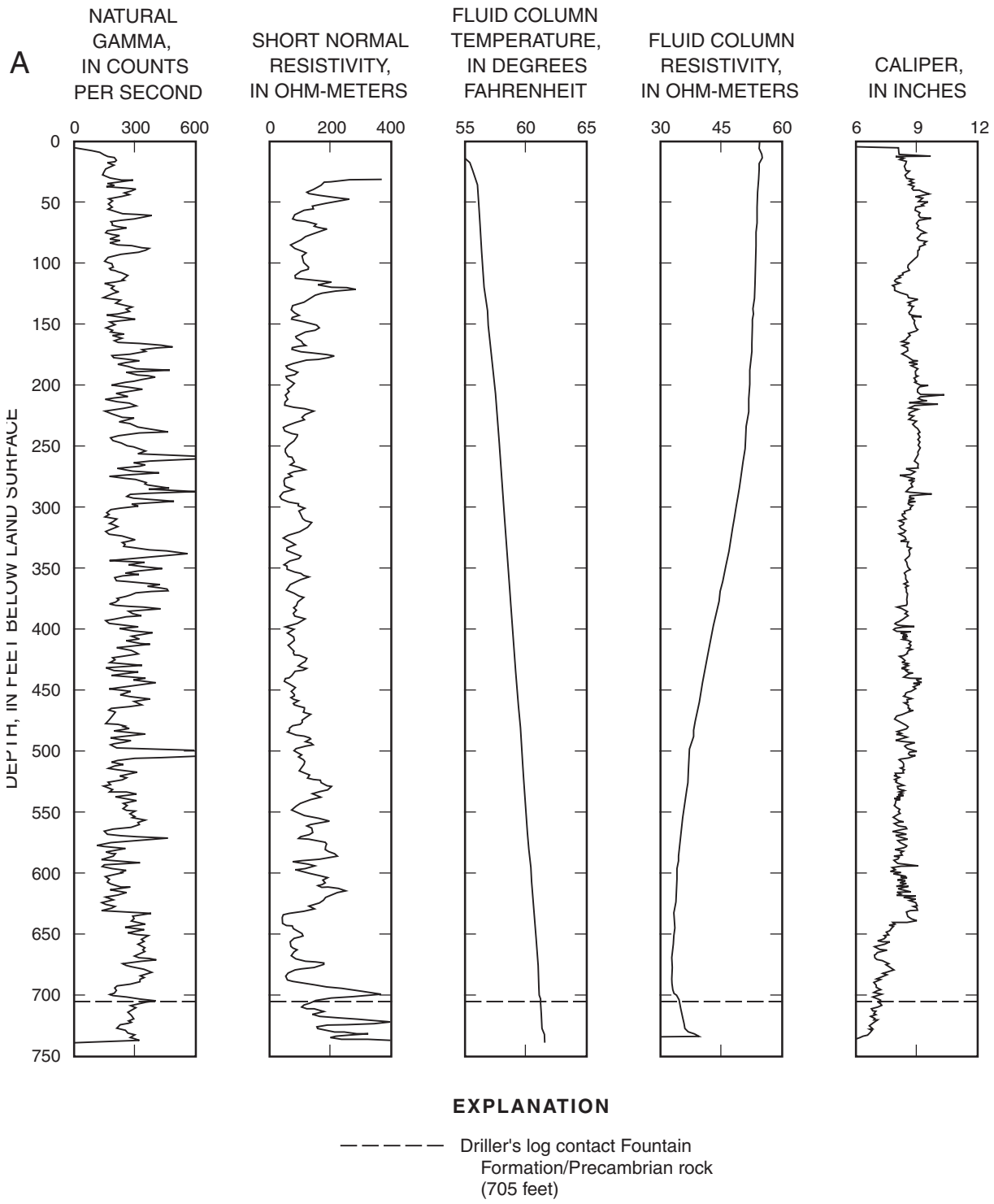

Figure 5. Geophysical logs for borehole LGMW-001-P: (A) composite of gamma, short-normal resistivity, fluid-column temperature and resistivity, and caliper logs; and (B) plot of borehole deviation giving coordinates of borehole offset from true vertical as a function of depth.

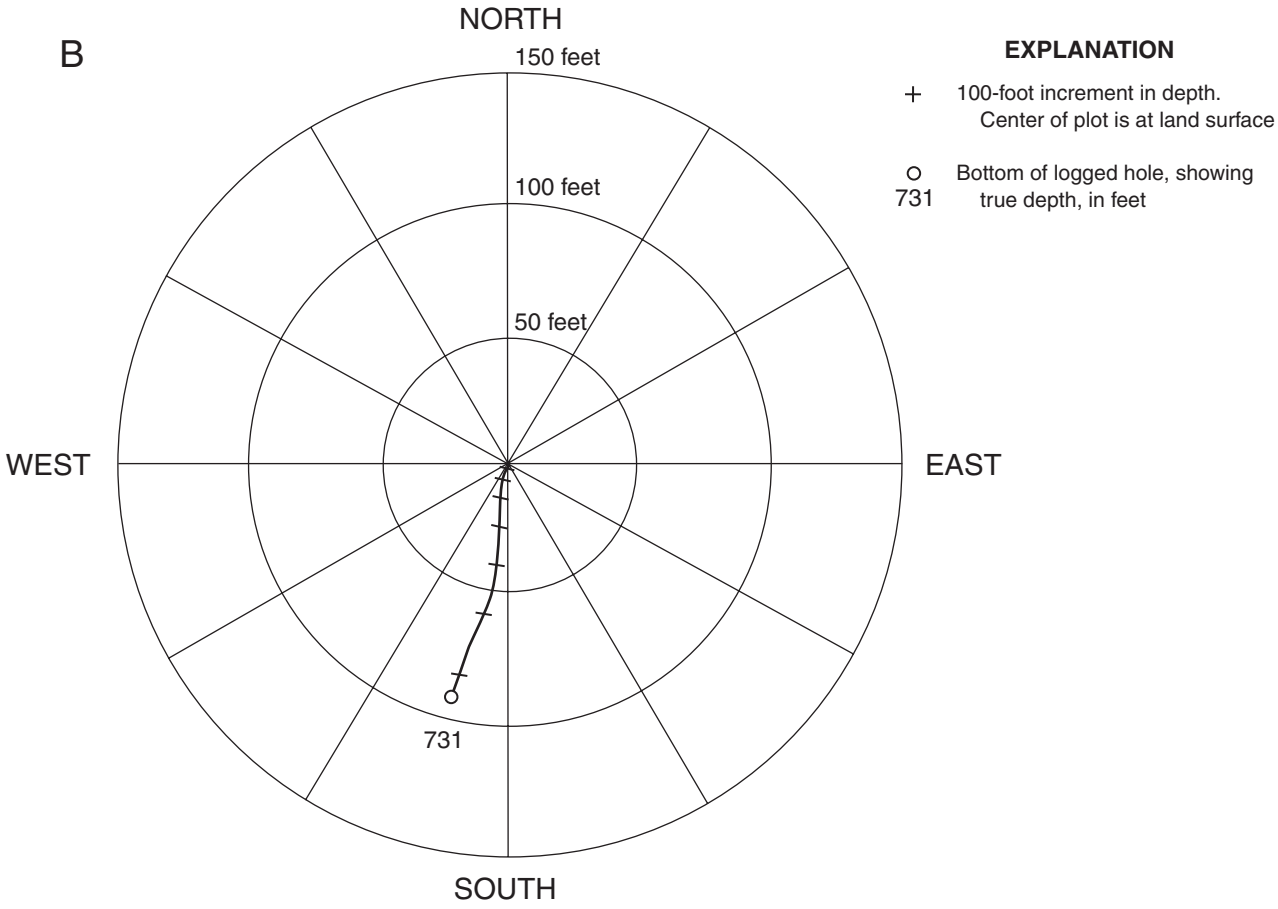

Figure 5. Geophysical logs for borehole LGMW-001-P: (A) composite of gamma, short-normal resistivity, fluid-column temperature and resistivity, and caliper logs; and (B) plot of borehole deviation giving coordinates of borehole offset from true vertical as a function of depth—Continued.

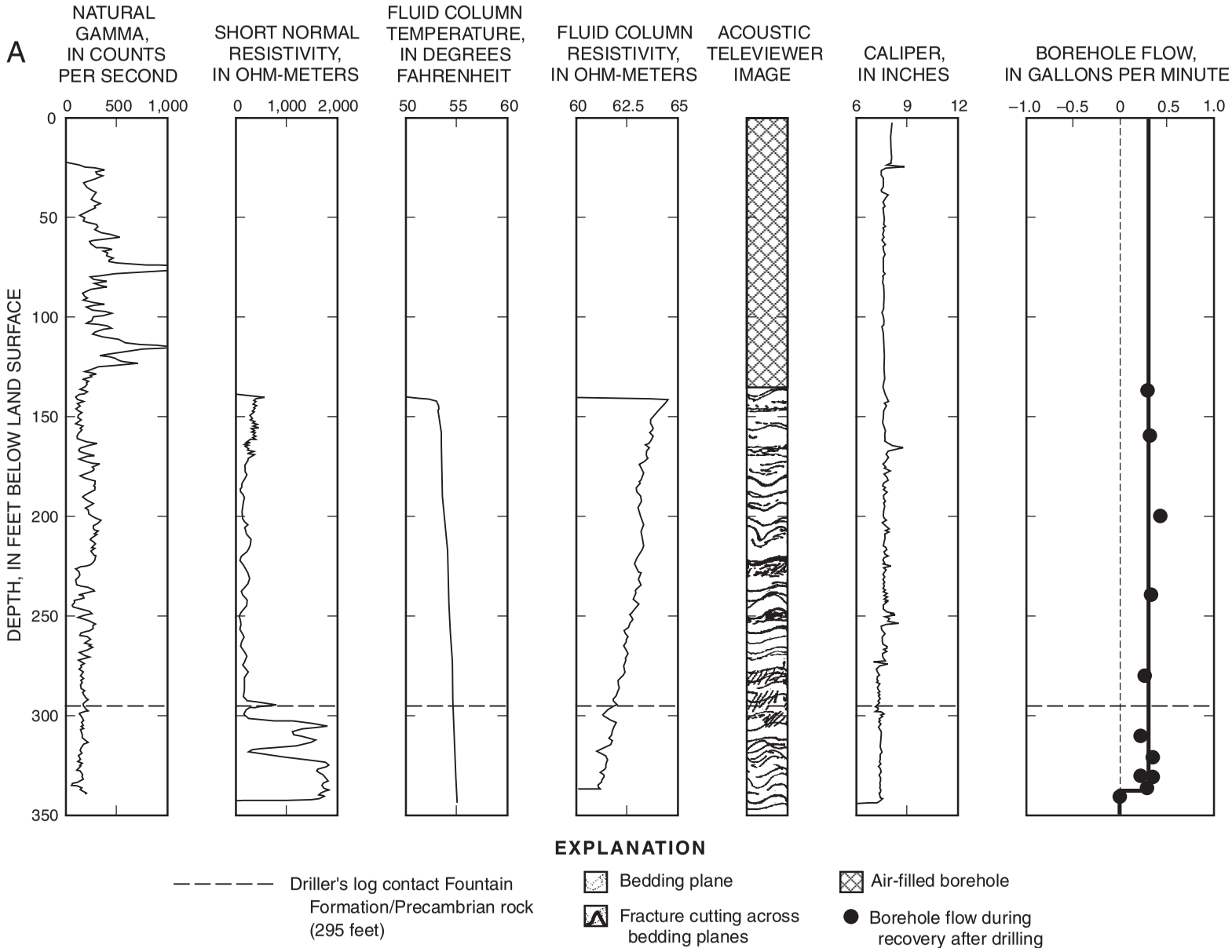

Figure 6. Geophysical logs for borehole LGMW-003-P: (A) composite of gamma, short-normal resistivity, fluid-column temperature and resistivity, televiewer, caliper, and flowmeter logs; and (B) plot of borehole deviation giving coordinates of borehole offset from true vertical as a function of depth.

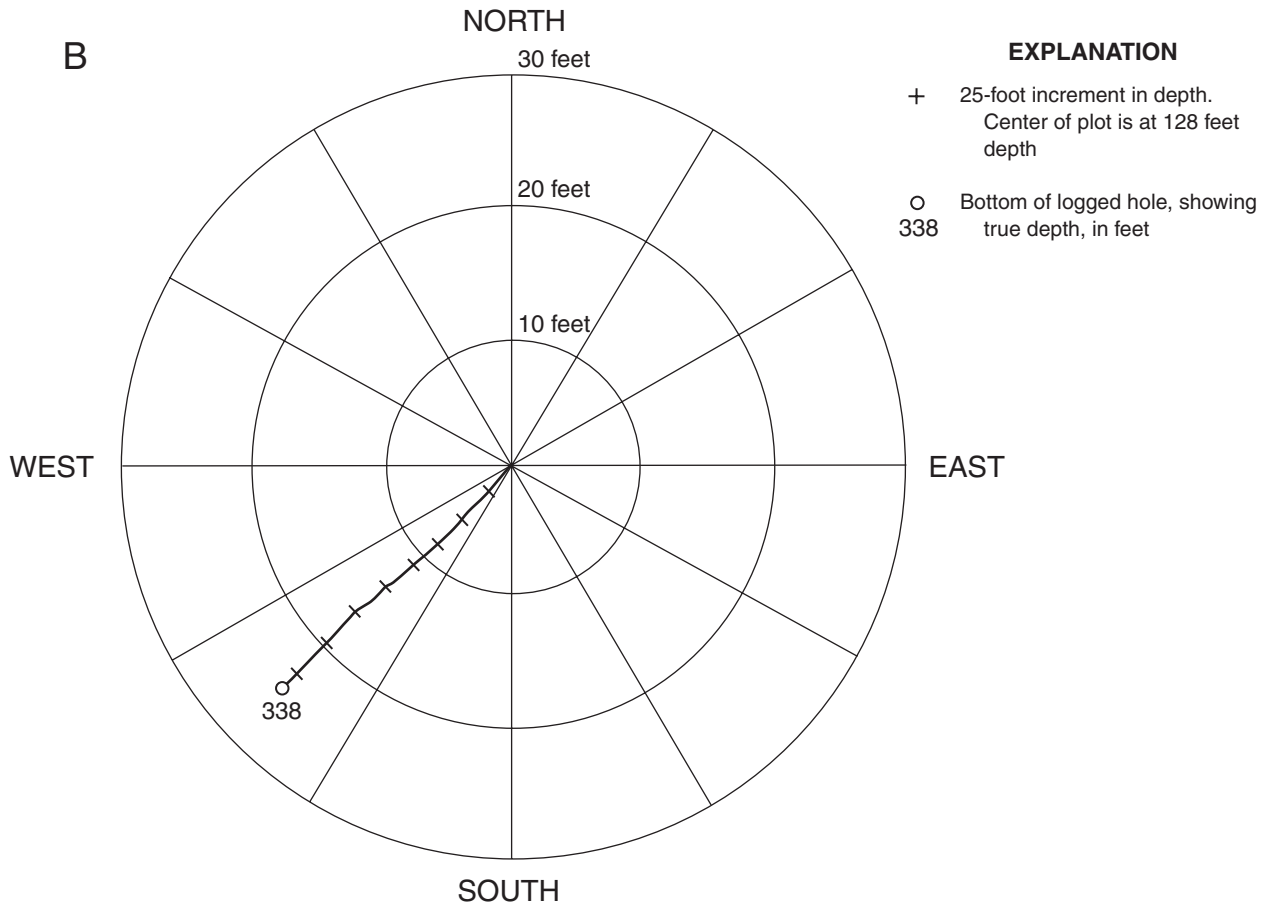

Figure 6. Geophysical logs for borehole LGMW-003-P: (A) composite of gamma, short-normal resistivity, fluid-column temperature and resistivity, televiewer, caliper, and flowmeter logs; and (B) plot of borehole deviation giving coordinates of borehole offset from true vertical as a function of depth—Continued.

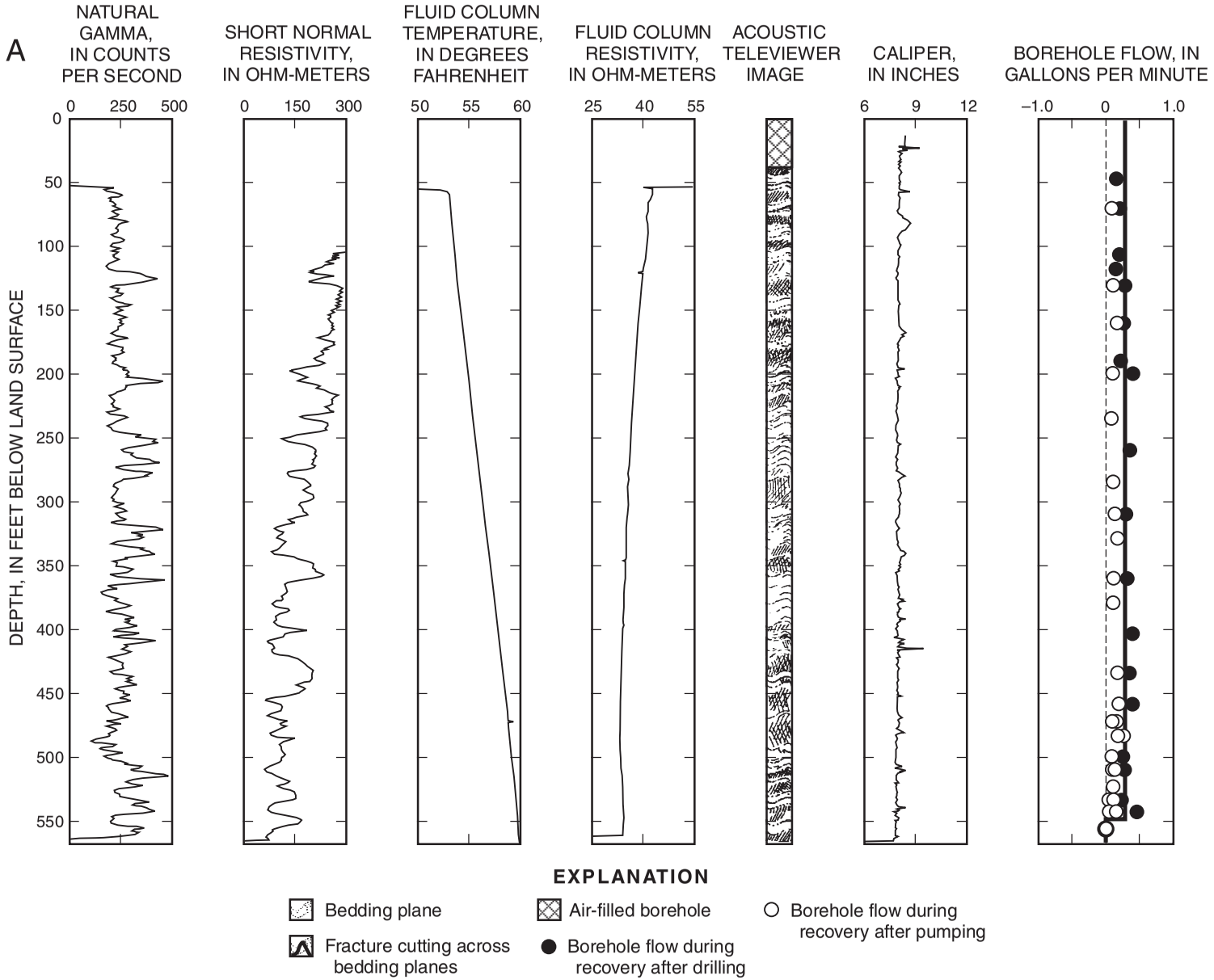

Figure 7. Geophysical logs for borehole LGMW-004-F: (A) composite of gamma, short-normal resistivity, fluid-column temperature and resistivity, televiewer, caliper, and flowmeter logs; and (B) plot of borehole deviation giving coordinates of borehole offset from true vertical as a function of depth.

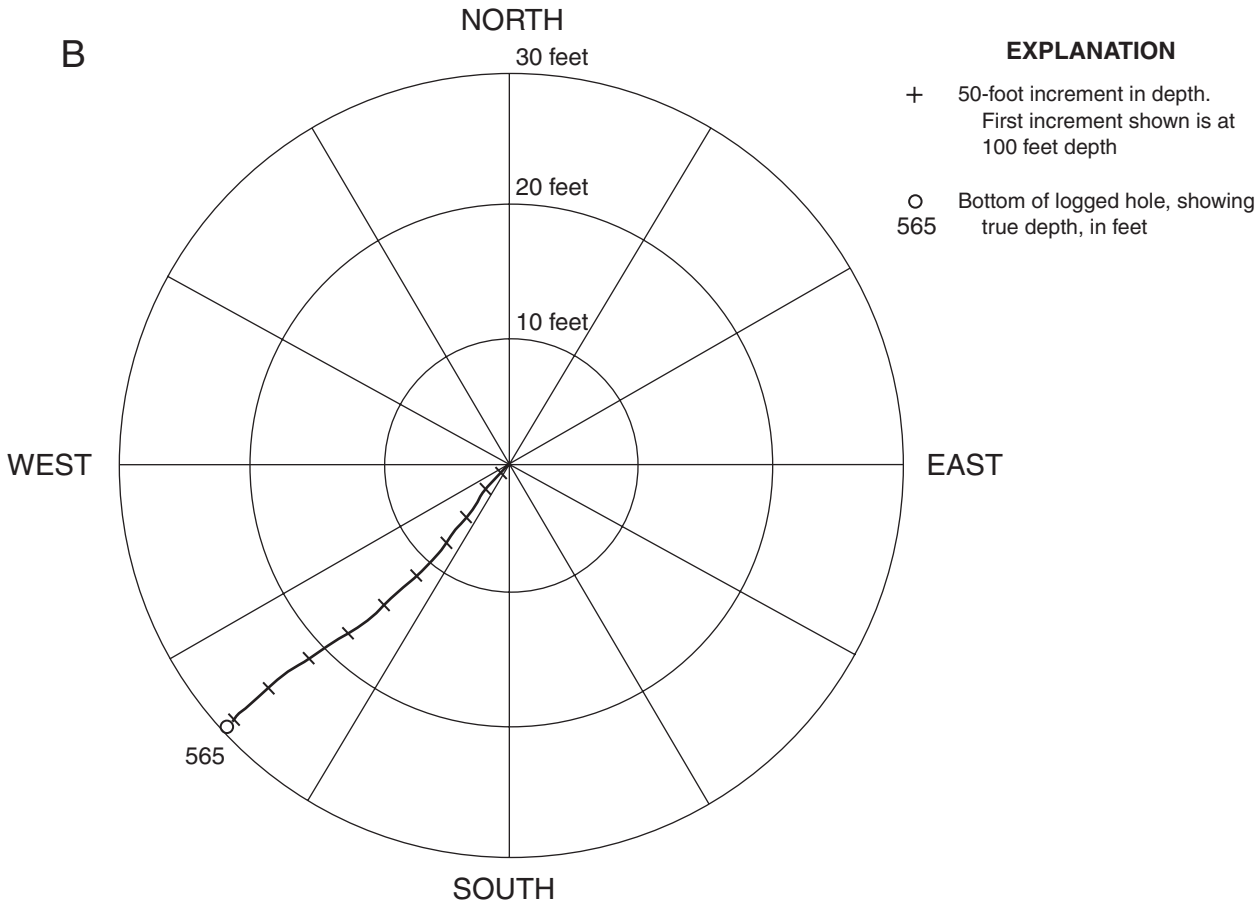

Figure 7. Geophysical logs for borehole LGMW-004-F: (A) composite of gamma, short-normal resistivity, fluid-column temperature and resistivity, televiewer, caliper, and flowmeter logs; and (B) plot of borehole deviation giving coordinates of borehole offset from true vertical as a function of depth—Continued.

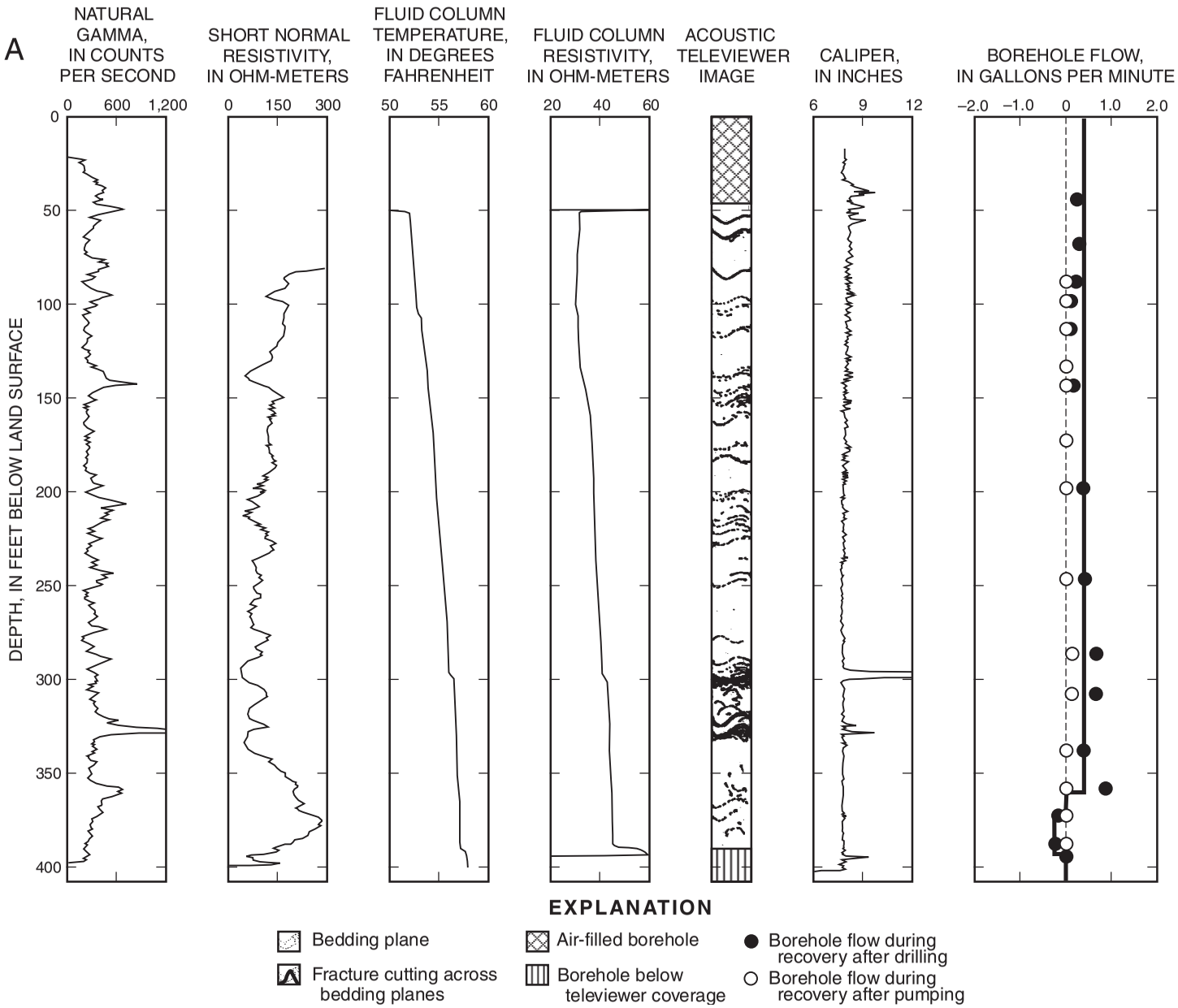

Figure 8. Geophysical logs for borehole LGMW-006-P: (A) composite of gamma, short-normal resistivity, fluid-column temperature and resistivity, televiewer, caliper, and flowmeter logs; and (B) plot of borehole deviation giving coordinates of borehole offset from true vertical as a function of depth.

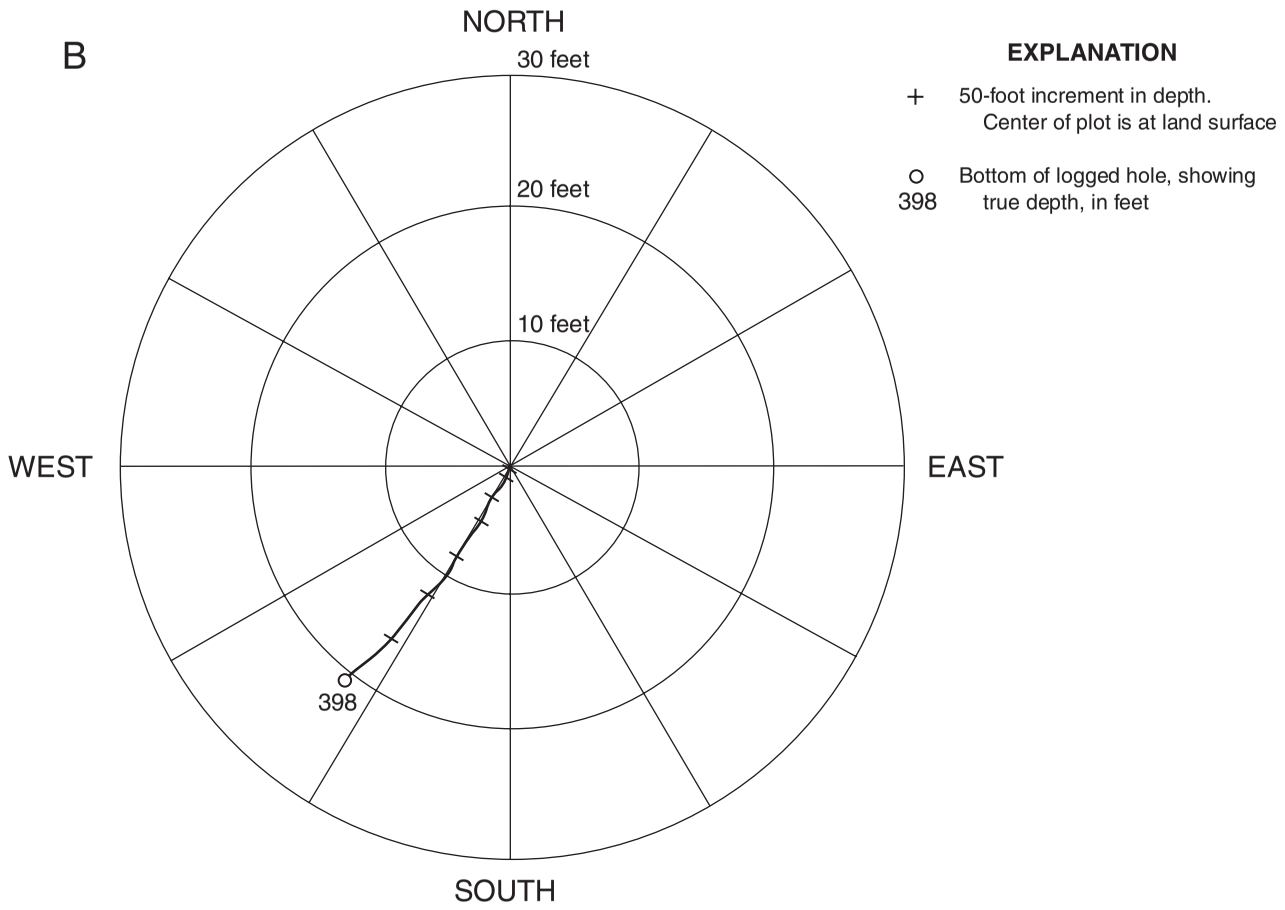

Figure 8. Geophysical logs for borehole LGMW-006-P: (A) composite of gamma, short-normal resistivity, fluid-column temperature and resistivity, televiewer, caliper, and flowmeter logs; and (B) plot of borehole deviation giving coordinates of borehole offset from true vertical as a function of depth—Continued.

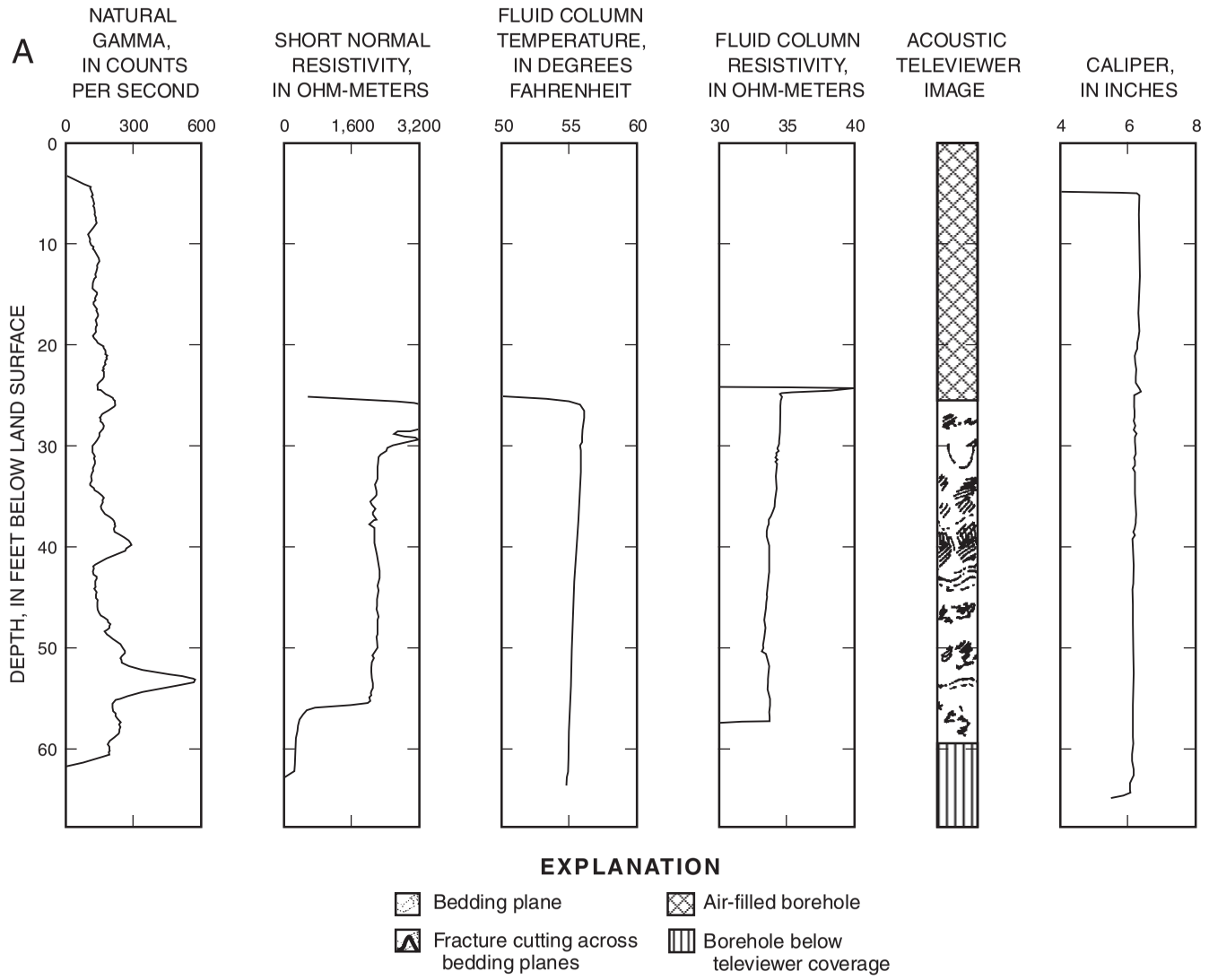

Figure 9. Geophysical logs for borehole LGMW-010-F: (A) composite of gamma, short-normal resistivity, fluid-column temperature and resistivity, televiewer, and caliper logs; and (B) plot of borehole deviation giving coordinates of borehole offset from true vertical as a function of depth.

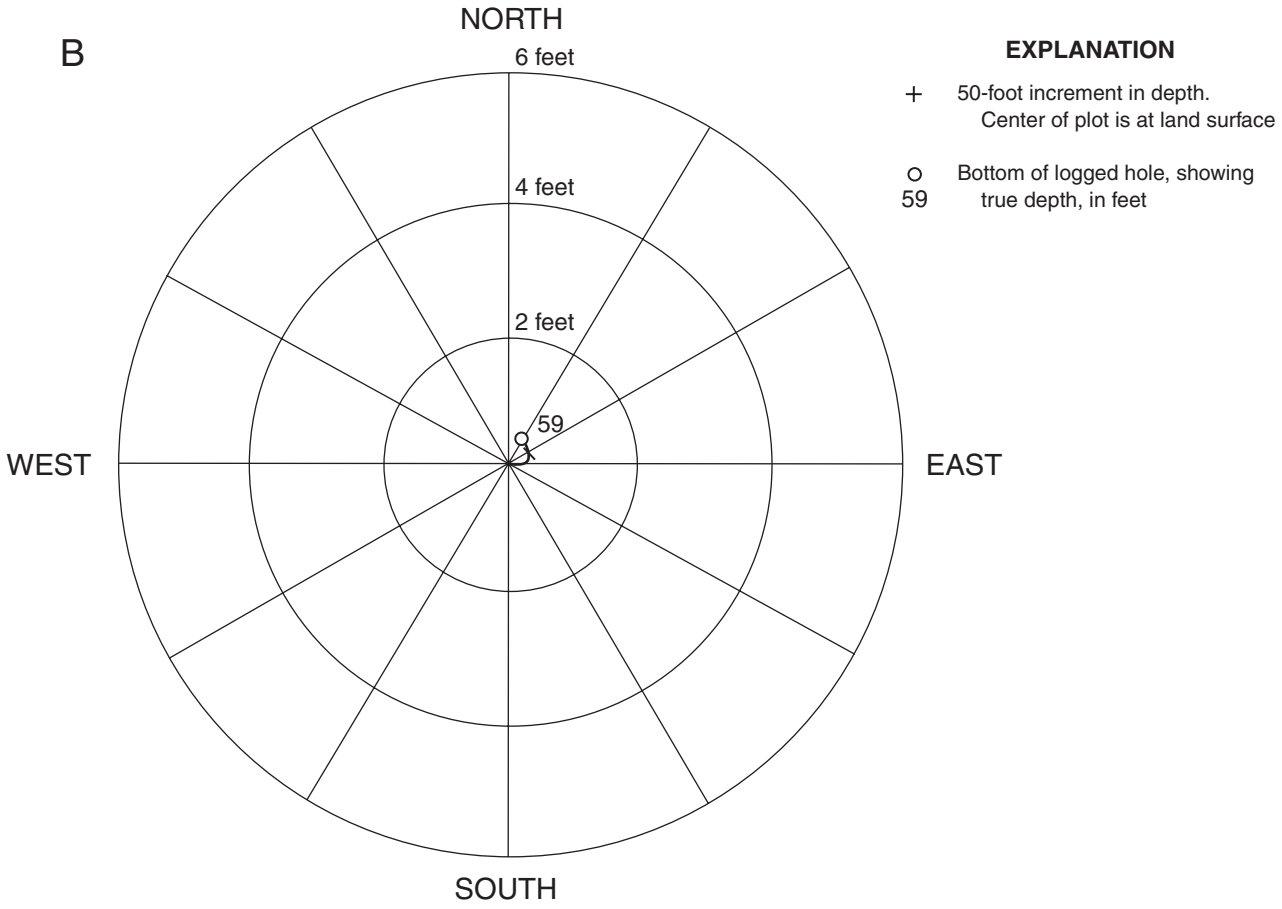

Figure 9. Geophysical logs for borehole LGMW-010-F: (A) composite of gamma, short-normal resistivity, fluid-column temperature and resistivity, televiewer, and caliper logs; and (B) plot of borehole deviation giving coordinates of borehole offset from true vertical as a function of depth—Continued.

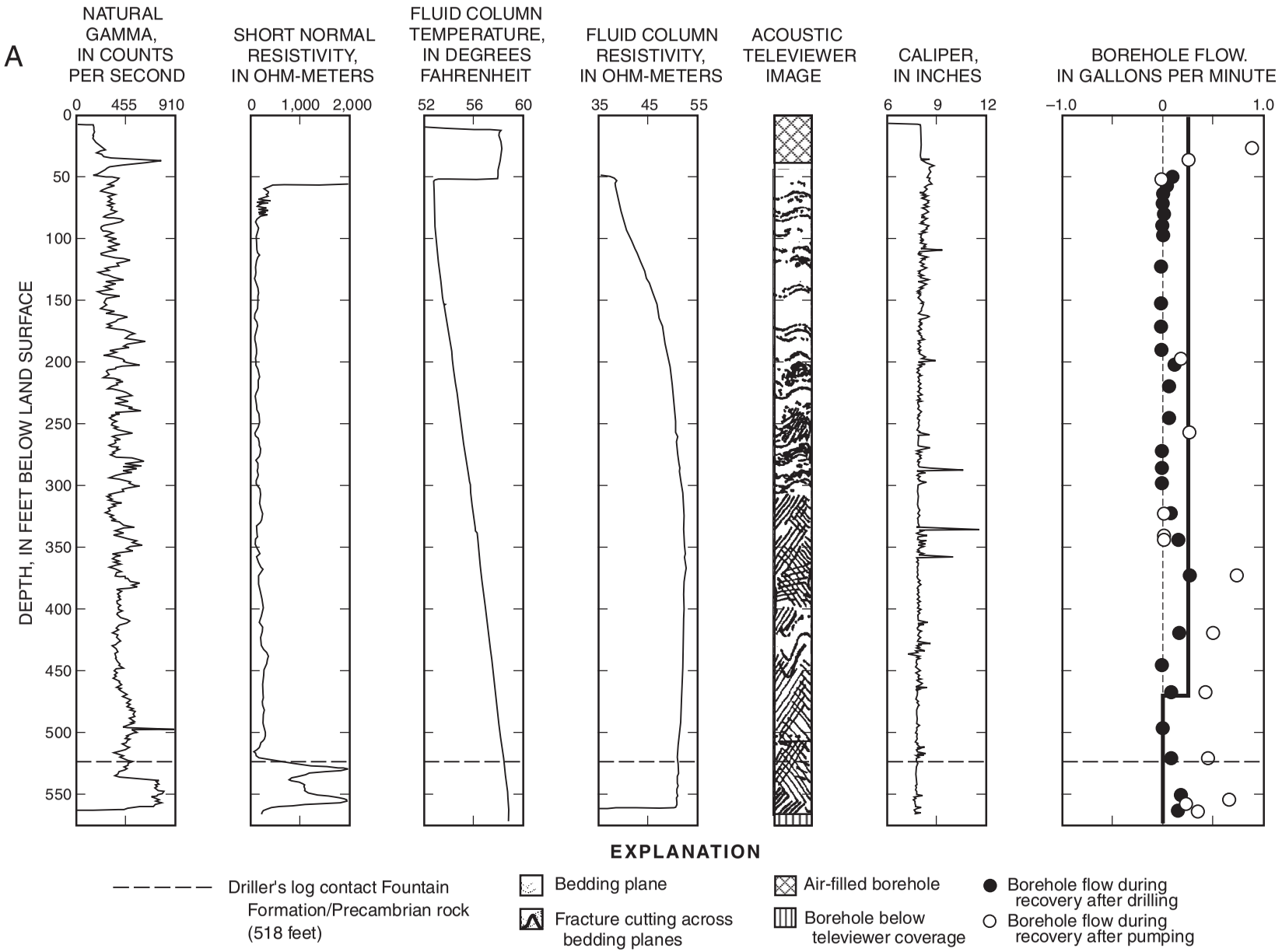

Figure 10. Geophysical logs for borehole LGMW-017-P: (A) composite of gamma, short-normal resistivity, fluid-column temperature and resistivity, televiewer, caliper, and flowmeter logs; and (B) plot of borehole deviation giving coordinates of borehole offset from true vertical as a function of depth.

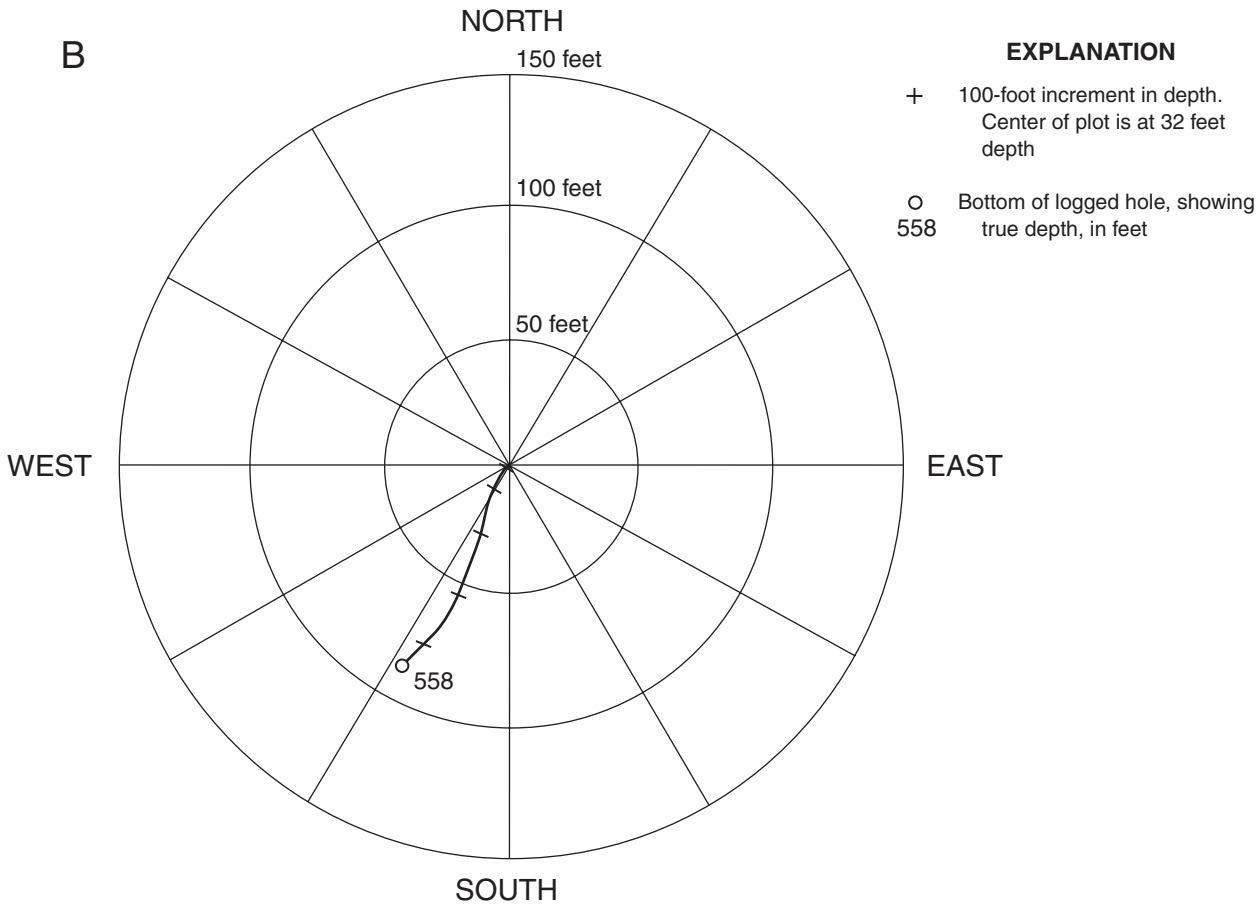

Figure 10. Geophysical logs for borehole LGMW-017-P: (A) composite of gamma, short-normal resistivity, fluid-column temperature and resistivity, televiewer, caliper, and flowmeter logs; and (B) plot of borehole deviation giving coordinates of borehole offset from true vertical as a function of depth—Continued.

Table 2. Stratigraphic strike and dip of the Fountain Formation from televiewer logs

[Depth is in feet below land surface; azimuths are in degrees clockwise from north]

Depth	Dip (degrees)		Strike azimuth (degrees)
	Angle	Azimuth	
	LGMW-001-P		
	No useful data for strike and dip		
	LGMW-003-P		
137.7	57.0	140.9	50.9
142.5	20.0	122.8	32.8
142.7	18.1	90.9	0.9
147.5	48.0	71.9	341.9
148.1	15.4	303.0	213.0
155.1	30.0	85.5	355.5
163.2	32.1	112.0	22.0
165.4	17.5	116.0	26.0
167.3	66.0	8.6	278.6
169.7	21.1	163.4	73.4
170.7	25.5	109.2	19.2
173.6	20.5	166.4	76.4
176.1	56.7	215.9	125.9
179.7	46.2	59.4	329.4
183.8	26.4	39.8	309.8
188.5	30.4	218.4	128.4
188.9	40.8	187.5	97.5
194.1	51.9	189.1	99.1
199.3	47.7	218.1	128.1
201.7	47.7	179.6	89.6
202.7	48.6	176.0	86.0
203.9	65.1	187.8	97.8
205.0	47.4	72.1	342.1
205.6	64.7	59.3	329.3
206.6	76.8	57.7	327.7
207.5	60.2	198.6	108.6
218.8	35.4	79.0	349.0
220.0	21.9	62.3	332.3
224.2	69.0	73.2	343.2
233.1	39.4	80.2	350.2
235.7	45.7	91.8	1.8
236.2	42.4	75.4	345.4
237.2	22.2	68.9	338.9
238.6	43.2	82.1	352.1
240.4	46.5	49.0	319.0
241.0	64.1	47.5	317.5
241.5	40.6	69.3	339.3
245.4	54.3	69.6	339.6
246.6	37.8	68.4	338.4

Table 2. Stratigraphic strike and dip of the Fountain Formation from televiewer logs—Continued

[Depth is in feet below land surface; azimuths are in degrees clockwise from north]

Depth	Dip (degrees)		Strike azimuth (degrees)
	Angle	Azimuth	
247.2	53.1	53.3	323.3
249.7	53.6	96.0	6.0
251.1	65.8	79.1	349.1
252.0	41.2	78.0	348.0
	LGMW-003-P–Continued		
256.4	41.5	72.9	342.9
256.7	50.9	59.1	329.1
260.8	48.6	61.2	331.2
263.5	39.4	40.6	310.6
264.0	50.2	76.5	346.5
266.1	52.0	71.5	341.5
266.5	48.0	76.8	346.8
267.9	39.5	54.8	324.8
269.2	76.3	54.2	324.2
274.2	31.1	333.3	243.3
275.2	56.9	348.7	258.7
281.1	59.4	7.2	277.2
285.9	41.2	87.6	357.6
Average	43.4	129.2	339.9
	LGMW-004-F		
97.0	67.5	96.9	6.9
121.5	69.9	82.4	352.4
179.5	62.9	84.6	354.6
188.5	62.8	86.8	356.8
204.0	65.3	79.7	349.9
214.0	52.6	89.3	359.3
140.5	65.5	74.4	344.4
165.0	59.2	73.7	343.7
172.5	57.7	68.8	338.8
278.0	62.9	85.1	355.1
324.5	61.8	83.3	353.3
363.0	60.2	89.5	359.5
373.5	59.5	86.0	356.0
385.5	63.4	86.8	356.8
394.0	60.2	82.4	352.4
397.5	63.0	74.5	344.5
429.0	60.0	76.5	346.5
442.0	64.8	76.3	346.3
444.0	74.0	95.1	5.1
461.0	68.8	79.1	349.1
463.5	63.3	75.8	345.8
473.0	63.1	67.7	337.7
491.0	53.0	92.9	2.9

Table 2. Stratigraphic strike and dip of the Fountain Formation from televiewer logs—Continued

[Depth is in feet below land surface; azimuths are in degrees clockwise from north]

Depth	Dip (degrees)		Strike azimuth (degrees)
	Angle	Azimuth	
516.0	61.6	88.3	358.3
522.5	55.4	83.4	353.4
537.5	57.8	84.0	354.0
558.0	54.1	78.8	348.8
Average	61.4	82.3	352.3
	LGMW-006-P		
44.9	50.2	81.6	351.6
48.2	69.5	74.5	344.5
55.3	69.8	67.7	337.7
56.7	71.6	66.2	336.2
58.4	67.5	63.5	333.5
59.4	68.9	69.0	339.0
78.6	63.0	72.0	342.0
91.5	67.9	59.8	329.8
97.0	52.0	71.7	341.7
141.4	67.0	81.2	351.2
171.0	63.5	70.5	340.5
209.4	67.9	44.9	314.9
218.6	58.6	62.2	332.2
219.2	62.1	45.9	315.9
221.4	69.5	100.3	10.3
222.2	61.7	94.2	4.2
225.8	67.1	69.1	339.1
244.2	65.2	76.1	346.1
269.5	59.9	91.0	1.1
275.8	64.4	41.1	311.1
281.1	63.6	104.8	14.8
283.8	65.5	75.0	345.0
287.3	51.9	100.3	10.3
289.2	61.6	91.7	1.7
292.0	67.8	87.9	357.9
Average	63.9	74.5	344.5
	LGMW-010-F		
35.0	51.3	100.0	10.0
46.5	49.0	121.2	31.2
39.0	56.8	107.2	17.2
Average	52.4	109.5	19.5
	LGMW-017-P		
No useful data			

Table 3. Strike and dip of fractures from televiewer logs

[Depth is in feet below land surface; azimuths are in degrees clockwise from north]

Depth	Dip (degrees)		Strike azimuth (degrees)
	Angle	Azimuth	
		LGMW-001-P	
111.8	61.4	74.4	344.4
122.5	70.7	83.7	353.7
473.9	65.3	78.3	348.3
		LGMW-003-P	
No fractures detected			
		LGMW-004-F	
No fractures detected			
		LGMW-006-P	
45.0	42.3	55.3	325.3
48.0	188.7	201.7	111.7
55.3	192.8	205.8	115.8
78.5	186.8	199.8	109.8
81.2	308.1	321.1	231.1
96.2	214.7	227.7	137.7
219.0	47.5	60.5	330.5
222.0	75.8	88.8	358.8
289.9	74.2	87.2	357.2
294.2	56.6	69.6	339.6
324.6	47.2	60.2	330.2
329.2	72.6	85.6	355.6
		LGMW-010-F	
No fractures detected			
		LGMW-017-P	
117.7	34.4	47.4	317.4
147.7	52.6	65.6	335.6
159.1	50.7	63.7	333.7
164.9	69.5	82.5	352.5
169.7	57.0	70.0	340.0
177.4	39.8	52.8	322.8
224.5	58.3	71.3	341.3
278.4	62.6	75.6	345.6
361.4	20.8	33.8	303.8
452.4	87.9	100.9	10.9
538.1	61.7	74.7	343.7
539.4	58.2	71.2	341.2

Table 4. Water-level measurements during logging

[Time is in hours and minutes in 24-hour (military) format; depth is feet below land surface]

	Time	Depth
LGMW-001-P		
No data		
LGMW-003-P		
During recovery after dewatering by drilling		
	09:53	139.40
	11:09	132.90
	12:17	127.95
LGMW-004-F		
A. During recovery after dewatering by drilling		
	11:33	55.47
	12:30	49.95
	13:43	43.43
	14:51	39.53
	14:56	38.97
	15:05	38.35
	15:24	37.17
	15:47	35.78
	16:03	34.85
	16:16	34.10
	16:33	33.20
	16:47	32.49
B. During recovery after pumping (pump off at 17:12)		
	17:14	60.58
	17:26	58.77
	17:41	56.64
	18:01	54.26
	18:20	52.21
	18:40	50.27
	19:00	48.42
	19:20	46.70
	19:39	45.37
LGMW-006-P		
A. During recovery after dewatering by drilling		
	09:13	64.19
	10:22	55.10
	11:15	52.00
	13:33	42.55
	14:25	39.93
B. During recovery after pumping (pump off at 14:38)		
	15:07	60.28
	15:22	57.32
	15:42	53.35

Table 4. Water-level measurements during logging—Continued

[Time is in hours and minutes in 24-hour (military) format; depth is feet below land surface]

	Time	Depth
	15:55	51.55
LGMW-010-F		
A. During recovery after dewatering by drilling		
	13:27	26.20
	14:20	26.20
	14:56	25.90
	15:20	25.96
B. During recovery after pumping (pump off at 15:36)		
	15:39	30.95
	15:42	30.53
	15:46	30.29
	15:50	30.23
	15:56	30.13
	16:02	29.97
	16:13	29.61
	16:20	29.60
	16:30	29.46
LGMW-017-P		
During recovery after dewatering by drilling		
	10:20	77.75
	11:28	68.34
	11:53	65.20
	12:32	60.60
	13:02	57.00
	13:32	53.93
	13:40	53.15
	15:10	43.87
	17:44	32.17
	18:14	29.98
	18:44	27.89
	19:07	26.55

Table 5. Heat-pulse-flowmeter data

[Depth is in feet below land surface; time is in hours and minutes in 24-hour (military) format; s, seconds; gpm, gallon per minute; >, greater than; <, less than]

Depth	Time	ΔT[1] (s)	Measured flow[2] (gpm)	Drawdown[3] (feet)	Drawdown-normalization factor[4]	Corrected flow[5] (gpm)
LGMW-001-P						
No data						
LGMW-003-P						
A. During recovery after dewatering by drilling						
137	11:33	2.2	0.1622	81.00	0.3	0.240
160	11:35	2.2	0.1622	80.70	0.3	0.240
200	11:39	1.4	0.2570	80.40	0.3	0.385
240	11:42	1.7	0.2110	80.10	0.3	0.315
280	11:46	2.3	0.1550	79.80	0.3	0.235
310	11:49	3.1	0.1140	79.50	0.3	0.170
320	11:53	1.9	0.1884	79.20	0.3	0.285
330	11:56	2.0	0.1788	79.00	0.3	0.270
340	11:59	>30.0	<0.01	78.80	0.3	<0.015
335	12:02	2.3	0.1550	78.40	0.3	0.235
330	12:06	2.9	0.1884	78.00	0.3	0.285
LGMW-004-F						
A. During recovery after dewatering by drilling						
47	15:04	20.9	0.0136	11.87	2.1	0.143
70	15:10	15.1	0.0203	11.67	2.1	0.213
69	15:14	16.5	0.0183	11.50	2.2	0.201
107	15:19	16.8	0.0179	11.35	2.2	0.197
130	15:23	12.9	0.0245	11.23	2.3	0.282
117	15:31	21.6	0.0130	10.97	2.3	0.150
160	15:36	14.1	0.0220	10.80	2.3	0.253
200	15:41	9.5	0.0345	10.65	2.3	0.397
189	15:49	17.6	0.0169	10.37	2.4	0.203
260	15:53	10.9	0.0296	10.23	2.4	0.355
310	15:57	15.5	0.0218	10.05	2.5	0.273
360	16:04	14.2	0.0242	9.87	2.5	0.303
404	16:06	13.0	0.0309	9.82	2.5	0.386
435	16:12	10.5	0.0276	9.64	2.6	0.359
460	16:16	11.6	0.0279	9.47	2.6	0.363
500	16:20	17.6	0.0169	9.33	2.7	0.228
510	16:27	15.7	0.0194	9.10	2.7	0.262
544	16:32	10.2	0.0319	8.93	2.8	0.447
535	16:39	20.1	0.0144	8.53	2.9	0.209
558	16:44	>25	<0.01	8.10	3.1	<0.150
B. During recovery after pumping (pump off at 17:12)						
558	17:13	>25	<0.01	35.30	0.7	<0.04
544	17:14	17.1	0.0175	35.00	0.7	0.062

Table 5. Heat-pulse-flowmeter data—Continued

[Depth is in feet below land surface; time is in hours and minutes in 24-hour (military) format; s, seconds; gpm, gallon per minute; >, greater than; <, less than]

Depth	Time	ΔT[1] (s)	Measured flow[2] (gpm)	Drawdown[3] (feet)	Drawdown-normalization factor[4]	Corrected flow[5] (gpm)
			LGMW-004-F—Continued			
535	17:18	18.6	0.0107	33.50	0.7	0.038
510	17:24	10.7	0.0303	32.50	0.8	0.121
500	17:28	14.3	0.0217	32.40	0.8	0.087
485	17:32	6.0	0.0570	31.45	0.8	0.228
473	17:37	14.4	0.0215	29.20	0.9	0.097
544	17:59	9.5	0.0346	28.30	0.9	0.156
535	18:03	14.1	0.0220	27.80	0.9	0.099
524	18:08	13.9	0.0224	27.20	0.9	0.101
510	18:10	13.2	0.0238	27.00	0.9	0.107
500	18:14	19.6	0.0148	26.40	0.9	0.070
485	18:18	9.6	0.0342	26.20	1.0	0.171
473	18:23	11.5	0.0279	25.70	1.0	0.140
460	18:25	8.7	0.0381	25.50	1.0	0.191
435	18:29	10.3	0.0316	25.10	1.0	0.158
380	18:36	14.7	0.0216	24.40	1.0	0.108
360	18:39	14.5	0.0213	23.10	1.1	0.117
330	18:43	10.9	0.0296	23.70	1.1	0.163
310	18:47	14.4	0.0215	23.30	1.1	0.118
285	18:55	17.0	0.0176	22.50	1.1	0.097
235	18:59	19.0	0.0154	22.20	1.1	0.085
200	19:02	17.5	0.0170	21.80	1.1	0.094
160	19:08	12.1	0.0264	21.35	1.2	0.158
130	19:14	19.3	0.0156	20.80	1.2	0.094
69	19:29	25.1	0.0107	19.60	1.3	0.070
			LGMW-006-P			
A. During recovery after dewatering by drilling						
45	13:02	3.9	0.0898	34.8	0.7	0.314
70	13:08	3.6	0.0976	34.2	0.7	0.342
90	13:10	4.7	0.0739	33.8	0.7	0.259
100	13:14	16.5	0.0183	33.4	0.7	0.064
115	13:22	16.6	0.0181	33.0	0.8	0.063
145	13:29	7.5	0.0448	32.6	0.8	0.179
200	13:41	3.0	0.1179	32.2	0.8	0.472
250	13:48	2.6	0.1366	31.8	0.8	0.546
290	13:52	1.7	0.2110	31.2	0.8	0.844
310	13:54	1.8	0.1991	30.7	0.8	0.796
340	13:57	4.0	0.0875	30.0	0.8	0.350
390	14:05	-5.4	-0.0715	29.7	0.8	-0.286
396	14:11	>20.0	<0.01	29.4	0.8	<0.04
360	14:16	1.6	0.2244	29.2	0.8	0.897
375	14:21	>20.0	<0.01	28.7	0.8	<0.04

Table 5. Heat-pulse-flowmeter data—Continued

[Depth is in feet below land surface; time is in hours and minutes in 24-hour (military) format; s, seconds; gpm, gallon per minute; >, greater than; <, less than]

Depth	Time	ΔT[1] (s)	Measured flow[2] (gpm)	Drawdown[3] (feet)	Drawdown-normalization factor[4]	Corrected flow[5] (gpm)
			LGMW-006-P—Continued			
B. During recovery after pumping (pump off at 14:38)						
390	15:02	-8.2	-0.0484	51.2	0.5	-0.121
375	15:04	>20.0	<0.01	50.7	0.5	<0.03
360	15:07	>20.0	<0.01	50.3	0.5	<0.03
340	15:09	>20.0	<0.01	49.8	0.5	<0.03
310	15:11	2.6	0.1366	49.3	0.5	0.342
290	15:14	2.3	0.1550	48.8	0.5	0.388
250	15:18	>20.0	<0.01	48.3	0.5	<0.03
200	15:21	4.3	0.0811	47.8	0.5	0.203
175	15:25	5.3	0.0651	47.3	0.5	0.163
145	15:28	>20.0	<0.01	46.7	0.5	<0.03
135	15:31	>20.0	<0.01	46.2	0.5	<0.03
115	15:32	15.4	0.0199	45.6	0.5	0.049
100	15:37	>20.0	<0.01	45.0	0.6	<0.03
90	15:41	19.0	0.0154	44.3	0.6	0.046
			LGMW-010-F			
No data						
			LGMW-017-P			
During recovery after dewatering by drilling						
569	11:39	4.3	0.0811	56.8	0.4	0.162
557	11:40	3.9	0.0898	56.5	0.4	0.180
525	11:47	8.6	0.0386	55.8	0.4	0.077
500	11:53	>20	<0.01	55.1	0.5	<0.025
470	11:55	8.9	0.0372	54.8	0.5	0.093
450	12:00	>20	<0.01	54.1	0.5	<0.025
425	12:04	4.8	0.0722	53.6	0.5	0.181
375	12:12	3.6	0.0976	52.0	0.5	0.244
350	12:18	6.3	0.0541	51.3	0.5	0.135
325	12:25	14.0	0.0222	50.6	0.5	0.056
305	12:34	>20	<0.01	49.9	0.5	<0.025
290	12:37	>20	<0.01	49.4	0.5	<0.025
275	12:41	>20	<0.01	48.8	0.5	<0.025
250	12:43	17.5	0.0170	48.3	0.5	0.043
225	12:49	15.5	0.0197	47.9	0.5	0.049
195	12:57	>20	<0.01	47.3	0.5	<0.025
201	13:00	8.0	0.0418	47.0	0.5	0.104
175	13:04	>20	<0.01	46.6	0.5	<0.025
155	13:10	>20	<0.01	46.0	0.5	<0.025
125	13:16	>20	<0.01	45.2	0.6	<0.030
100	13:19	>20	<0.01	44.8	0.6	<0.030
92	13:22	>20	<0.01	44.2	0.6	<0.030

Table 5. Heat-pulse-flowmeter data—Continued

[Depth is in feet below land surface; time is in hours and minutes in 24-hour (military) format; s, seconds; gpm, gallon per minute; >, greater than; <, less than]

Depth	Time	ΔT[1] (s)	Measured flow[2] (gpm)	Drawdown[3] (feet)	Drawdown-normalization factor[4]	Corrected flow[5] (gpm)
			LGMW-017-P—Continued			
88	13:24	>20	<0.01	44.0	0.6	<0.030
75	13:28	>20	<0.01	43.7	0.6	<0.030
70	13:32	>20	<0.01	43.5	0.6	<0.030
60	13:36	16.0	0.0190	42.9	0.6	0.057
55	13:39	14.0	0.0222	42.5	0.6	0.067
569	17:30	5.9	0.0581	22.7	1.1	0.320
557	17:43	9.3	0.0354	21.8	1.1	0.195
557	17:48	3.4	0.1036	21.4	1.2	0.621
525	18:03	4.5	0.0773	20.8	1.2	0.464
470	18:09	4.9	0.0707	20.3	1.2	0.424
425	18:16	4.6	0.0755	19.8	1.3	0.491
375	18:24	3.1	0.1140	19.4	1.3	0.741
350	18:28	>20	<0.01	19.1	1.3	<0.065
345	18:32	>20	<0.01	18.8	1.3	<0.065
355	18:34	>20	<0.01	18.5	1.3	<0.065
325	18:38	>20	<0.01	18.2	1.4	<0.070
250	18:44	10.1	0.0323	17.9	1.4	0.226
202	18:49	11.5	0.0279	17.6	1.4	0.195
75	18:59	16.6	0.0181	17.3	1.4	0.127
55	19:03	>20	<0.01	17.0	1.5	<0.0705
30	19:07	3.2	0.1103	16.7	1.6	0.882
40	19:09	11.7	0.0274	16.3	1.6	0.219
55	19:12	>20	<0.01	15.9	1.6	<0.080

[1]Heat-pulse-response time, given as the average of three or more consecutive measurements recorded after any initial trend in heat-pulse magnitude.

[2]Flow response based on flow-column calibrations in smooth-walled laboratory environment; positive flows are upward and negative flows are downward.

[3]Drawdown estimated to each flow-measurement time by fitting a smoothed curve to discrete water-level measurements and projecting water level to an approximate steady-state level.

[4]Normalization factor based on projecting measured flow to the flow at 25 feet of drawdown; rounded off to nearest tenth because of the approximate nature of the normalization.

[5]Flow multiplied by 5.0 bypass factor established for heat-pulse flowmeter in rough-walled boreholes similar to those at Lariat Gulch, as verified by field calibration, and normalized to flow expected at 25 feet of drawdown.

Borehold LGMW-001-P

No flowmeter data are available for this well, and no water-level-recovery data were available because the well was flowing at top of casing. The televiewer log is not shown because the mudcake on the walls obscured the image along most of the borehole; fracture information is summarized in table 3. Available logs are shown in figure 5A.

Borehole LGMW-003-P

All inflow (water flowing into the borehole) was unambiguously attributed to a single, relatively tight (transmissivity less than 2 feet squared per day [ft^2/d]) feature (stratum or fracture) near the bottom of the borehole at a depth between 335 and 340 feet (fig. 6A). Lack of significant inflow indicates low permeability in the vicinity of the contact between the Fountain Formation and the Precambrian rock. The short normal resistivity log indicates that the top of crystalline rock is at a depth of about 295 feet. The televiewer image of bedding planes in the Fountain Formation shows variation in strike and dip with depth, and many of the planes appear to depart from the expected image of the intersection of a dipping plane with the borehole; the beds appeared contorted, more like foliation than bedding.

Borehole LGMW-004-F

All inflow appears to enter the borehole below 550 feet, and no other inflow zones were indicated by the fluid-column temperature or resistivity logs (fig. 7A). Bedding planes within the Fountain Formation appear to dip consistently eastward at about 60 degrees, generally striking about 10 degrees west of north (table 2).

Borehole LGMW-006-P

This borehole (fig. 8A), though drilled to a depth of about 462 feet, could only be logged to a maximum depth of about 402 feet (caliper log) because of an obstruction in the borehole at that depth; therefore logging did not extend to the contact between the Fountain Formation and the Precambrian crystalline rocks, which is at a depth of about 410 feet, according to the driller's log (Marsha Bates, Shaw Group, Inc., written commun., 2002). Most inflow appears to enter the borehole just below a depth of 360 feet. The identification of downflow (water flowing down the borehole) at a depth of about 390 feet indicates a bedding plane fracture or thin permeable bed with lower hydraulic head below that depth. The measured flow rates and the observed rate of recovery after drilling indicate that all inflow zones are of low permeability (transmissivity less than 2 ft^2/d). A conspicuous borehole enlargement at a depth of about 300 feet is so highly altered and damaged by drilling that no strike or dip can be assigned. Two borehole enlargements at depths of about 325 and 330 feet clearly are fractures dipping to the east. On the basis of the flowmeter data, neither of these fractures have substantial permeability. The fluid-column logs indicate an outflow (water flowing out of the borehole) zone for the weak down-flow at about 392 feet. Fluid-column logs do not indicate the inflow zone in the 370- to 385-foot interval because water entering at that depth flows upward and downward, causing no change in water quality at the inflowing fracture. The fluid-column logs indicate no measurable inflow from the pair of dipping fractures at about 325 and 330 feet, but indicate some weak inflow occurred at the borehole enlargement

near 300 feet, and additional weak inflow occurred at the 130- to 150-foot interval. Even with all of these inflow points, total borehole transmissivity is estimated to be less than 2 ft^2/d.

Borehole LGMW-010-F

This borehole (fig. 9A) is shallow (about 65 feet deep) with very little measurable inflow and no clearly defined inflow point. Flowmeter data (not shown in fig. 9A) gave spurious results, varying from no measurable flow to upflow as great as 3 gpm. Flowmeter data were rejected because, in the judgment of the senior author, the data indicated convective overturning of the fluid column and not true vertical flow. Convective overturning was indicated by low formation permeability, short borehole length, small total drawdown, and logging immediately after drilling; drilling causes thermal disequilibrium in the formation, which drives convective overturning. Water production during recovery probably was equal to the average of 0.2 gpm determined from the slow rise in water level.

Borehole LGMW-017-P

All inflow came from below a depth of 560 feet (fig. 10A). The fluid-column logs did not provide any indication of other inflow points. The televiewer log provided limited information for stratigraphic strike and dip of the Fountain Formation because of a mudcake along most of the borehole wall (table 2); fracture information is summarized in table 3.

Overview of Lariat Gulch Logs

In the deeper boreholes, the combination of gamma and short-normal resistivity logs indicates a bedded Fountain Formation with relatively high gamma counts and relatively low resistivity in more shaley intervals. However, differentiation between sand and shale in the sequence is not as direct as it is for most sedimentary rocks because of local concentrations of naturally occurring uranium within the rock and relatively unweathered, feldspar-rich rock fragments in the arkosic sandstone intervals. Therefore, the gamma and resistivity logs indicate bedding within the Fountain Formation, but a simple and direct relation between either resistivity or gamma activity and lithology probably cannot be given. In the case of two boreholes that were drilled through the Fountain Formation and into crystalline basement rocks (LGMW-003-P and LGMW-017-P), the contact is shown as an abrupt shift to higher formation resistivity (figs. 6A and 10A).

The number of features judged to be bedding planes (table 2) or fractures (table 3) varies widely among the boreholes, depending on the texture of the borehole wall, the bedding within the formation, and the effects of borehole environment and natural mud in the drilling fluid on the quality of the televiewer-log image. The average strike and dip of these bedding planes (corrected for borehole deviation and magnetic declination) (table 2) show considerable variation, ranging over about 43–64 degrees for dip, and from about 21 degrees west of north clockwise to about 20 degrees east of north for strike. These variations probably represent local shifts in the structure of the Fountain Formation that result from deformation and uplift along the western margin of the Denver Basin. Boreholes LGMW-003-P and LGMW-006-P show substantial variation in the orientation of strike and dip. Otherwise, the strike and dip of beds given in table 2 are consistent with the steeply eastward-dipping nature of Fountain Formation beds at the Lariat Gulch site.

The very low values of measured flow make interpretation of flowmeter logs difficult. With the nominal flow-measurement resolution of the flowmeter of 0.01 gpm (Hess, 1986) multiplied by a bypass factor of 5.0, the

resolution of the data set is about 0.05 gpm, a major fraction of the recovery rate in the boreholes. Thus, much of the scatter in the data results from the flow shifting into and out of the effective measurement range.

Other reasons that made flowmeter-log data difficult to model were that (1) only the deepest inflow zones could be identified, and (2) the logs were not run at true steady-state conditions. The simplest approach is to simulate the recovery as if it were steady upflow at an average drawdown equal to the upflow as indicated by both the measured borehole flow and the average rate of water-level recovery multiplied by the 2.6-gallon-per-foot volume of the 8-inch borehole. Transmissivity values estimated by this approach (table 6) ranged from about 0.5 to 1.85 ft^2/d. These transmissivity estimates indicate that the permeability of any sandstone beds, bedding-plane openings, or fractures intersecting the boreholes is very low—fully two orders of magnitude less than permeabilities determined for fractures in intensively fractured rock at Mirror Lake in New Hampshire (Paillet and others, 1987; Paillet, 1998) and Raymond Quarry in California (Karasaki and others, 2000).

Table 6. Summary of heat-pulse-flowmeter results

[Depth is in feet below land surface; gpm, gallon per minute; ft^2/d, feet squared per day; –, no data]

Borehole	Depth of primary inflow zone	Average drawdown (feet)	Recovery rate (gmp)	Transmissivity estimate (ft^2/d)
LGMW-001-P	–	–	–	–
LGMW-003-P	335-340	80	0.21	0.50
LGMW-004-F	550-560	20	0.25	1.85
LGMW-006-P	300-360	25	0.20	1.40
LGMW-010-F	30-60	10	0.08	1.45
LGMW-017-P	560-600	35	0.25	1.30

SUMMARY AND CONCLUSIONS

Six boreholes at the Lariat Gulch site were logged with a suite of gamma, normal-resistivity, fluid-column temperature and resistivity, caliper, televiewer and heat-pulse-flowmeter probes. The log data were analyzed to identify fractures and bedding planes and to help determine the contact between the sedimentary Fountain Formation and the underlying Precambrian crystalline rock. The logs indicated relatively few fractures intersecting the boreholes. None of these fractures are estimated to have transmissivity values greater than 2 ft^2/d. Water-producing zones were of such low transmissivity in the Lariat Gulch boreholes that the high-resolution heat-pulse flowmeter could barely detect upflow during water-level recovery after drilling. The scatter in the flowmeter data was so great that crossflow (vertical movement of flow in the borehole from one water-producing zone to another) could not be positively identified. But the trends in the flow data combined with inflections in the fluid-column temperature and resistivity logs suggested that some crossflow may exist, especially in the case of borehole LGMW-006-P, where downflow was measured in the lower part of the borehole. However, the hydraulic head difference associated with this one definite case of crossflow could not be estimated. The scatter in the data also identified the deepest water-producing zone to be the bottom of the upflow regime during recovery, but other water-producing zones may exist in the interval above those deepest zones. However, the transmissivity of these upper zones cannot be more than a fraction of the low average transmissivity (always less than 2 ft^2/d) estimated for each borehole. Although the quality of the flowmeter-log data

makes log interpretation difficult in this study, previous results with the same suite of logs in similar geological formations under similar logging conditions leave little doubt that if highly transmissive features such as bedding planes or fractures intersected the six Lariat Gulch boreholes, those features would have been detected.

REFERENCES CITED

American Society for Testing and Materials, 1995, Standard guide for planning and conducting borehole geophysical logging: American Society for Testing and Materials, Philadelphia, D–5753, 8 p.

Hearst, J.R., Nelson, P.H., and Paillet, F.L., 2000, Well logging for physical properties: New York, John Wiley, 483 p.

Hess, A.E., 1986, Identifying hydraulically conductive fractures with a slow velocity borehole flowmeter: Canadian Journal of Earth Sciences, v. 23, p. 69–78.

Hodges, R.E., 1988, Calibration and standardization of geophysical well-logging equipment for hydrologic applications: U.S. Geological Survey Water-Resources Investigations Report 88–4058, 25 p.

Hodges, R.E., and Teasdale, W.E., 1991, Considerations related to drilling methods in planning and performing borehole-geophysical logging for ground-water studies: U.S. Geological Survey Water-Resources Investigations Report 91–4090, 17 p.

Jorgensen, D.G., 1991, Estimating geohydrologic properties from corehole geophysical logs: Ground Water Monitoring and Remediation, v. 10, no. 2, p. 123–129.

Karasaki, K., Freifield, B., Cohen, A., Grossenbacher K., Cook, P., and Vasco, D., 2000, A multidisciplinary characterization study at Raymond field site, Raymond, California: Journal of Hydrology, v. 236, no. 1, p. 17–34.

Keys, W.S., 1986, Analysis of geophysical well logs with a microcomputer: Ground Water, v. 24, no. 6, p. 750–760.

Keys, W.S., 1990, Borehole geophysics applied to ground-water investigations: U.S. Geological Survey Techniques of Water-Resources Investigations, book 2, chap E2, 150 p.

Kwader, Thomas, 1985, Estimating aquifer permeability from formation resistivity factors: Ground Water, v. 23, no. 5, p. 762–766.

McCary, L.M., 1980, Use of geophysical logs to estimate water-quality trends in carbonate aquifers: U.S. Geological Survey Water-Resources Investigations Report 80–57, 29 p.

Molz, F.J., Morin, R.H., Hess, A.E., Melville, J.G., and Guven, O., 1989, The impeller meter for measuring aquifer permeability variations – Evaluation and comparison with other tests: Water Resources Research, v. 25, no. 7, p. 1677–1683.

Morin, R.H., Hess, A.E., and Paillet, F.L., 1988, Determining the distribution of hydraulic conductivity in a fractured limestone aquifer by simultaneous injection and geophysical logging: Ground Water, v. 26, no. 5, p. 587–595.

Paillet, F.L., 1998, Flow modeling and permeability estimation using borehole flow logs in heterogeneous formations: Water Resources Research, v. 34, no. 5, p. 997–1010.

Paillet, F.L, 2000a, A field technique for estimating aquifer parameters using flow log data: Ground Water, v. 38, no. 4, p. 510–521.

Paillet, F.L, 2000b, Flow logging in difficult boreholes—Making the best of a bad deal, *in* International Symposium on Borehole Geophysics for Minerals, Geotechnical, and Groundwater Applications, 7th, Denver, Colo., 2000, Proceedings: Houston, Tex., The Minerals and Geotechnical Logging Society, A Chapter at Large of the Society of Professional Well Log Analysts, p. 125–135.

Paillet, F.L., 2001, Hydraulic head applications of flow logs in the study of heterogeneous aquifers: Ground Water, v. 39, no. 5, p. 667–675.

Paillet, F.L., and Crowder, R.E., 1996, A generalized approach for the interpretation of geophysical well logs in ground water studies—Theory and application: Ground Water, v. 34, no. 5, p. 883–898.

Paillet, F.L., Hess, A.E., Cheng, C.H., and Hardin, E.L., 1987, Characterization of fracture permeability with high-resolution vertical flow measurements during borehole pumping: Ground water, v. 25, no. 1, p. 28–40.

Paillet, F.L., Keys, W.S., and Hess, A.E., 1985, Effects of lithology on televiewer-log quality and fracture interpretation: Society of Professional Well Log Analysts Annual Logging Symposium, 26th, Dallas, Tex., 1985, Transactions, p. JJJ1–JJJ30.

Paillet, F.L., Lundy, James, Tipping, Robert, Runkel, Anthony, Reeves, Laurel, and Green, Jeffrey, 2000, Hydrogeologic characterization of six sites in southeastern Minnesota using borehole flowmeters and other geophysical logs: U.S. Geological Survey Water-Resources Investigations Report 00–4142, 33 p.

Paillet, F.L., Senay, Yildir, Mukhopadhyay, Amitabha, and Szekely, Ferenc, 2000, Flowmetering of drainage wells in Kuwait City, Kuwait: Journal of Hydrology, v. 234, p. 208–227.

Parsons Engineering Science, Inc., 1999a, Supplemental remedial investigation report for Air Force Plant PJKS, Colorado—v. IV: Denver, Colorado, prepared by Parsons Engineering Science, Inc., submitted to U.S. Army Corps of Engineers, Omaha District, March 1999, variously paginated.

Parsons Engineering Science, Inc., 1999b, Supplemental remedial investigation report for Air Force Plant PJKS, Colorado—v. I: Denver, Colorado, prepared by Parsons Engineering Science, Inc., submitted to U.S. Army Corps of Engineers, Omaha District, April 1999, variously paginated.

Williams, J.H., and Johnson, C.D., 2000, Borehole wall imaging with acoustic and optical televiewers for fractured bedrock aquifers, *in* International Symposium on Borehole Geophysics for Minerals, Geotechnical, and Groundwater Applications, 7th, Denver, Colo., 2000, Proceedings: Houston, Tex., The Minerals and Geotechnical Logging Society, A Chapter at Large of the Society of Professional Well Log Analysts, p. 43–53.

Zemanek, Joseph, Glenn, E.E., Norton, L.J., and Caldwell, R.L., 1970, Formation evaluation by inspection with the borehole televiewer: Geophysics, v. 35, p. 254–262.